



TECHNISCHE
UNIVERSITÄT
WIEN
Vienna University of Technology



D I P L O M A R B E I T

Vorbereitung biologischer Proben für Elektronen-Mikroskopie

Vergleich zwischen Chemischer Fixierung und Hoch-Druck
Frieren

Ausgeführt am Institut für

Angewandte Physik

der Technischen Universität Wien

unter der Anleitung von **Prof. Gerhard Schütz** in Zusammenarbeit mit

Dr. Thomas Heuser

durch

Katharina Susanne Keuenhof, B.Sc.

Reznicekgasse 10/9, 1090 Wien

13. Juli 2017

Katharina Keuenhof

Gerhard Schütz



MASTER'S THESIS

Preparation of Biological Specimens for Electron Microscopy

Comparison of Chemical Fixation and High-Pressure Freezing

Carried out at the Institute for

Applied Physics

of the Vienna University of Technology

under the supervision of **Prof. Gerhard Schütz** in collaboration with

Dr. Thomas Heuser

by

Katharina Susanne Keuenhof, B.Sc.

Reznicekgasse 10/9, 1090 Wien

13. July 2017

Katharina Keuenhof

Gerhard Schütz

Erklärung zur Verfassung der Arbeit

Katharina Susanne Keuenhof, B.Sc.

Reznicekgasse 10/9

A-1090 Wien

Hiermit erkläre ich, dass ich diese Arbeit selbstständig verfasst habe, dass ich die verwendeten Quellen und Hilfsmittel vollständig angegeben habe, dass ich die Stellen der Arbeit, – einschließlich Tabellen, Karten und Abbildungen – die anderen Werken oder dem Internet im Wortlaut oder dem Sinn nach entnommen sind, auf jeden Fall unter Angabe der Quelle als Entlehnung kenntlich gemacht habe.

13. Juli 2017

Katharina Susanne Keuenhof

Acknowledgements

I would like to express my gratitude to Thomas Heuser for giving me the opportunity to work with him and his team. I am extremely grateful to Marlene Brandstetter for supervising my project, Harald Kotisch for always lending a hand, Nicole Fellner and Sonja Jacob for helping me with anything else I needed. Overall, the entire team has been nothing but supportive, offering me answers to all my questions, endless shared coffees and most importantly their friendship. I am thankful to Andreas Walter for his company and for having kept me from becoming sane (you read that right). I would not have been able to freeze and fix anything, had I not been given specimens by fellow scientists. Those include Alexander Dammerman, Daniel Serwas, Anna Gschwandner, Dominik Handler, Jeroen Dobbelaere, Harald Kotisch and Anete Romanauska. My parents have very much supported me throughout my entire studies, and I am sure they too are happy those are coming to an end. Lastly thank you to my friends and roommates Maria Kozyrev, Alina Seiler and Alina Pšeničný for bearing (with) me during various stages of my thesis.

Zusammenfassung

Zur Anschauung ultrastruktureller Elemente in biologischen Materialien ist Elektronenmikroskopie unabdingbar. Die Proben müssen richtig präpariert werden, um dem Vakuum und der Strahlung innerhalb eines Elektronenmikroskopes widerstehen zu können. Der klassischste Ansatz ist eine chemische Fixierung. Fixative erhalten die Zellstruktur indem sie Verbindungen zwischen Proteinen und Lipiden herstellen und Schwermetalle werden zur Kontraststeigerung eingesetzt. Es ist eine einfache und kosteneffektive Prozedur die dem Hochdruck Frieren gegenüber steht. Während des Gefriervorgangs mittels flüssigem Stickstoff wird ein extrem hoher Druck ausgeübt um die Ausdehnung von Eiskristallen und somit eine Beschädigung der Probe zu verhindern. Die Probe wird anschließend einer Gefriersubstitution unterzogen bei der gefrorenes Wasser durch flüssige Lösungsmittel und Fixative ersetzt und langsam auf 0°C erwärmt wird. Die Wahl der Fixierungsmethode hängt von der Probe und der zu untersuchenden Struktur ab. Gewebe und Zellkulturen wurden mittels beiden Methoden präpariert und die Qualität der Ultrastruktur verglichen. In hochdruck-gefrorenen Proben waren Membranen deutlich glatter und Mitochondrien besser erhalten. Neuronale Komponenten waren in chemisch fixierten Proben besser fixiert, allerdings traten Fehler in der Einbettung häufiger auf.

Abstract

Electron microscopy (EM) is indispensable when it comes to the analysis of ultrastructural elements of biological material. However, the right preparation is necessary so that biological samples withstand vacuum and radiation inside an electron microscope without changes in ultrastructure. Chemical fixation can be considered the most classical approach. Fixatives are used to crosslink proteins as well as lipids to retain the original structure and stains are added for increased contrast. It is a relatively easy and cost effective procedure. On the other hand, high-pressure freezing offers a more physical approach to structural preservation. Exertion of a very high pressure during rapid freezing in liquid nitrogen hinders the expansion of ice crystals and thus the damage to cellular material. The sample subsequently undergoes a process called freeze substitution in which frozen water is replaced by liquid solvents and fixatives while slowly warming up to 0°C. The optimal method of preparation varies by sample and structure of interest. To establish a comparison, tissue and cell cultures from various organisms were prepared and the quality of the ultrastructure compared. High-pressure frozen samples typically showed smoother membranes and better preservation of mitochondria. Chemically fixed samples demonstrated better fixation of neuronal components but a higher likelihood of faulty resin infiltration.

Contents

1	Introduction	5
2	Aim	7
3	Theoretical Framework	10
3.1	Transmission Electron Microscopy	10
3.1.1	Production of the Electron Beam	12
3.1.2	Lenses in Electron Microscopes	13
3.1.3	Interactions of Electrons with Matter	14
3.1.4	Detection of Electrons	18
3.2	Sample preparation	18
3.2.1	Chemical fixation	19
3.2.2	HPF-FS	26
3.2.3	Embedding and Sectioning	30
3.2.4	Post-Staining	31
3.3	Specimens	33
3.3.1	<i>Caernohabditis elegans</i>	33
3.3.2	Cyanobacteria	34
3.3.3	<i>Drosophila melanogaster</i>	36
3.3.4	HeLa cells	37
3.3.5	NUP60 Yeast cells	37
4	Materials and Methods	38
4.1	<i>Caernohabditis elegans</i>	38
4.1.1	Chemical Fixation	38

4.1.2	HPF-FS	40
4.2	Cyanobacteria	41
4.2.1	Chemical Fixation	41
4.2.2	HPF-FS	42
4.3	<i>Drosophila</i> testis and wingdiscs	43
4.3.1	Chemical Fixation	43
4.3.2	HPF-FS	44
4.4	HeLa cells	45
4.4.1	Chemical Fixation	45
4.4.2	HPF-FS	46
4.5	NUP60 Yeast cells	47
4.5.1	Chemical Fixation	47
4.5.2	HPF-FS	48
5	Results	50
5.1	Comparison	50
5.1.1	<i>Caernohabditis elegans</i>	50
5.1.2	Cyanobacteria	52
5.1.3	<i>Drosophila melanogaster</i> – Testis	54
5.1.4	<i>Drosophila melanogaster</i> – Wingdiscs	55
5.1.5	HeLa Cells	56
5.1.6	NUP60 Yeast Cells	57
5.2	Artefacts	59
6	Discussion	60
7	Outlook	63

List of Abbreviations

AFS	Automatic Freeze-Substitution
BSA	Bovine Serum Albumin
CCD	Charge-Coupled Device
CF	Chemical Fixation
CB	Cytoskeleton Buffer
c/o	Condenser-Objective Lens
C1	Condenser Lens 1
C2	Condenser Lens 2
ddH₂O	Double-Distilled Water
DP	Diffraction Pattern
EM	Electron Microscopy
ER	Endoplasmic Reticulum
FS	Freeze Substitution
GA	Glutaraldehyde
HPF	High-Pressure Freezing/Freezer
HPV	Human Papilloma Virus
LaB₆	Lanthanum Hexaboride
LC	Lead Citrate
LN₂	Liquid Nitrogen
MeOH	Methanol
OsO₄	Osmium Tetroxide
OSC	Ovarian Somatic Cells
PBS	Phosphate Buffered Saline
RT	Room Temperature
SEM	Scanning Electron Microscopy
TEM	Transmission Electron Microscopy
UA	Uranyl Acetate
VBCF	Vienna Biocenter Core Facilities
W	Tungsten
W⁻	White Minus

1. Introduction

Electron microscopy allows the imaging of specimens with much higher resolution than optical light microscopy. Material sciences samples can be visualised at atomic resolution more easily than biological samples requiring extensive preparation. It is the latter that restricts the resolution to several nanometres in chemically fixed samples whereas other samples (e.g. viruses, protein complexes) have been visualised up to 0.2nm resolution by cryo-EM. Due to their content of water and radiation sensitivity, biological specimens need to be prepared in a much more extensive manner than other materials. The water needs to be removed, whilst keeping the ultrastructure intact. Different ways of preparing samples have been established, both with their own advantages and drawbacks. A "classical" approach to fixation is chemical fixation (CF). The specimen, be it tissue, cells or entire organisms that fulfill the size requirements, is fixed and stained using various chemicals before being dehydrated. High-pressure freezing (HPF) uses the process of vitrification to fix cellular structures almost instantaneously. Using a method called automated freeze substitution (FS), HPF-samples are then fixed at temperatures far below zero. Independent of the method of fixation, the specimens are subsequently dehydrated and embedded into resin blocks. Thin sections are cut off, deposited on a grid and stained before being observed in an electron microscope. The contrast in the observed images is subjected to several variables such as accelerating voltage, apertures, and specimen preparation. Different methods of observation are available, depending on the quality of the specimen and the area of interest. The most general approach is to use transmission electron microscopy (TEM) to achieve a two-dimensional (2D) image of the section. Additionally, 3D projections of the sample can

be produced using tomography methods. These contain more information and may allow a more detailed comparison of chemical fixation and HPF-FS. The goal is to determine whether one method is more favourable than the other depending on the visualised specimen and the relevant structure. Different structures and compositions may influence the quality and information content of the resulting images. One cell component may react differently than another to a certain method of fixation. Finding the most appropriate method of preparation for a specific sample is of great advantage when the goal is to be able to observe an organism in its original state.

2. Aim

High-pressure freezing was developed in 1968 by Moor and Riehle [1] and is continuously being more used. It has proven to generally provide better conservation of ultrastructural features, although this cannot necessarily be said for all types of samples. Compared to other cryofixation methods, such as plunge freezing, it allows effective freezing of much larger samples, of up to 500 μm in thickness. Different ultrastructural elements, especially when originating from a range of samples respond differently to chemical fixation or HPF-FS. Being able to use the best available protocol for sample preparation, reducing or even eliminating artefacts and representing the ultrastructure true to its form in a physiological environment is crucial. However, HPF requires costly equipment and more experienced personnel than CF. It is therefore valuable to establish an overview of which advantages exist and when HPF is preferable.

Comparisons have already been made for specific tissues, notably from Zechmann *et al.* [2], who compared the two methods regarding the effect of a virus on the ultrastructure of plant leaf cells. They note that cells fixed using cryopreservation methods had smoother membranes and that the cytosol had finer granulation than those fixed chemically. Additionally, they highlighted differences between media used in FS. Some were less effective at preserving finer structures, e.g. mitochondria, and did not provide enough membrane contrast.

Kiss *et al.* opted to use cryofixation of root tips to be able to preserve them in their entirety [3]. They also report smoother membranes, vacuoles containing electron dense material and improved conservation of microtu-

bules. Endoplasmic reticulum (ER) cisternae were wider than in chemically fixed samples and the resolution of Golgi intercisternal stacks was improved. In this paper, HPF was done without using cryoprotectants.

Germinating pea leaves were examined by Kaneko and Walther, who were able to preserve samples that were up to 200 μm thick without noticeable freeze damage [4]. Besides smoother membranes, they observed organelles that looked swollen compared to those fixed using CF. The latter showed consistent membrane stainability, as opposed to HPF samples.

Royer *et al.* made a comparison for the preservation of the ultrastructure in barbel taste buds of the catfish [5]. They report a higher regularity in the shape of intracellular organelles and also smoother-looking membranes. The final electron density and therefore contrast varied depending on the preparation method.

The two methods were also compared by Serwas and Dammermann for *Caenorhabditis elegans* [6]. The nematode provides a great example for hindrances that may be encountered during fixation. Larvae and adult worms possess a cuticle that is mainly impermeable to most chemicals, complicating adequate penetration and fixation. The embryos have an even less permeable egg shell which in some cases requires pre-treatment with sodium hypochlorite. The authors have found that fixation using HPF and FS allowed better ultrastructural preservation and eliminated the previously necessary permeabilization. Chemical fixation, however, provides images with higher contrast.

In 2002, Tsuyama *et al.* compared gastric gland component cells from rats [7]. They show adequate preservation up to a depth of 150 μm . Similarly to [5], immunostaining worked better with high-pressure frozen samples than chemically fixed ones.

This thesis will provide a detailed comparison for various types of specimens commonly used in EM labs. As opposed to previous studies, it covers a broader range of organisms and uses already elaborated protocols that are known to give the best achievable results. The protocols referred to in this work are also those used at the EM facility of the Vienna Biocenter Core Facilities (VBCF). The samples are currently involved in active research projects,

increasing their relevance for investigation on this topic. This work offers an explanation of the involved methods and a systematic comparison for various types of specimens.

3. Theoretical Framework

3.1 Transmission Electron Microscopy

Resolution of optical light microscopy is given by the Rayleigh criterion:

$$r = \frac{1.22\lambda}{2n \sin \theta}$$

r resolution [nm] λ wavelength of beam [nm]
 n refractive index θ half-angle of cone

It is therefore limited by the wavelength of visible light to around 200nm. The relationship between resolution and wavelength is the same for transmission electron microscopy. To overcome this restriction in resolution, accelerated electrons with shorter wavelengths can be used. The wavelength of the electron can be expressed using:

$$\lambda = \frac{h}{\sqrt{2m_0eV(1 + \frac{eV}{2m_0c^2})}}$$

λ wavelength [m] m_0 rest mass of an electron [kg]
 h Planck's constant [Nm·s] eV kinetic energy of the electron [J]

The equation above takes into account relativistic effects which make a significant difference starting electron energies of 100kV as the velocities surpass half the speed of light. The much shorter wavelength (down to picometers) allows for higher resolution. Figure 3.1 shows a visual representation of the Rayleigh criterion. Two different points are considered resolved as long

as they can be observed as two distinct points. A smaller wavelength allows the distinction of points that are closer together.

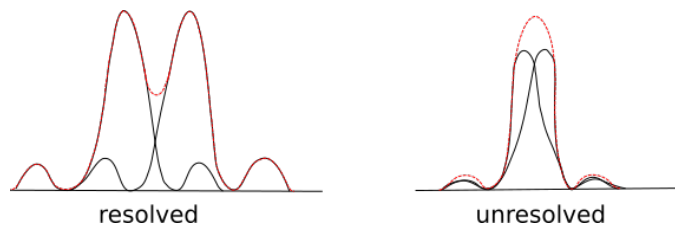


Figure 3.1: Left image shows two points sufficiently far apart to be distinguished as separate points. In the right image, the waves overlap and the two points are perceived as one.

Although photons and electrons differ in their interaction with matter, the latter remain very useful for image production. The optics of electrons are similar to those of light, which is why ray diagrams are also helpful here. Figure 3.2 shows the path of an electron beam through an electron microscope. After production of the electron beam, the condenser lens system is traditionally responsible for the production of a parallel beam. Condenser lens 1 (C1 lens) creates an image of the gun crossover. Depending on the size of the source in relation to the area that should be illuminated, condenser lens 2 (C2 lens) adjusts it by condensing or magnifying it. Underfocus of the C2 lens will give a more parallel beam than overfocus. In most TEMs, however, the C2 lens is focused and the upper objective lens, sometimes referred to as the C3 or condenser/objective (c/o) lens, produces a parallel beam at the level of the specimen plane. The C2 aperture is located right below the C2 lens and limits parts of the electron beam. It must be aligned correctly to ensure the beam and therefore the optical axis are centered with all further apertures and to avoid the image moving away from the axis and distorting when adjusting the C2 lens. The specimen is located underneath the upper pole piece of the c/o lens, and below it is the objective aperture. The latter limits electrons scattered at too large an angle, improving contrast. The lower objective lens is then responsible for magnification. The objective lens is the most powerful lens in the electron microscope. Further below, the first intermediate image is magnified again by the intermediate lens, producing

a second intermediate image. It is magnified one last time by the projector lens, and projected onto the viewing screen. To record images, a camera can be inserted below the last lens.

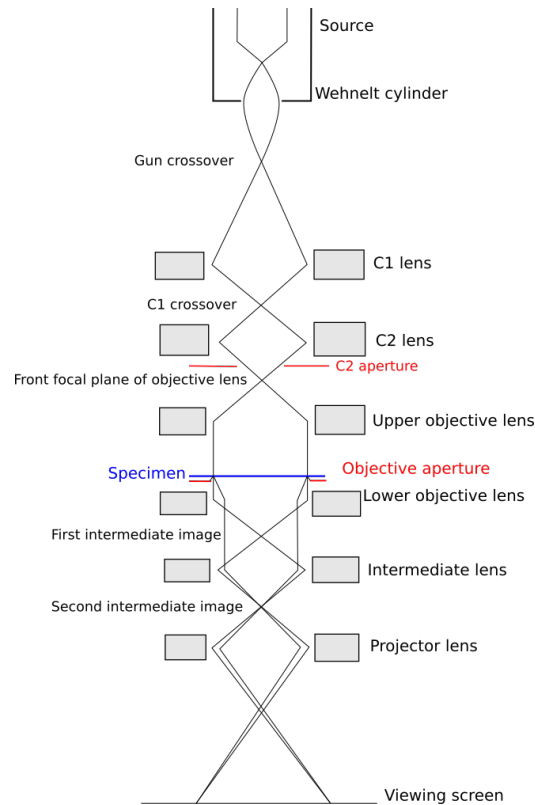


Figure 3.2: Ray diagram of an electron microscope. Electrons are scattered at the specimen, and some rays blocked by the objective aperture.

3.1.1 Production of the Electron Beam

To achieve good quality images, a reliable electron source is necessary. Two ways of producing electron beams are using either thermoionic sources or field-emission sources. Schottky sources combine both types.

Thermoionic sources are heated to provide the electrons in the material with an energy higher than their work function. This allows the electrons to escape the material. The energy required is about a few eV and would

cause most materials to melt. Tungsten (W) has a high enough melting point and low enough work function to be a suitable material used for thermoionic sources and is therefore used for filaments. Lanthanum hexaboride (LaB_6) crystals can also act as sources and have the advantage of having a lower working function, lower operating temperature and thus a longer lifetime.

Field Emission sources rely on a large potential difference between the source and an anode. Applying a certain voltage V to a so-called ‘tip’ results in a large electrical field E whose magnitude is inversely proportional for the size of the tip r : $E = \frac{V}{r}$. Due to the severe stress being imposed, the material requires high mechanical strength. Tungsten crystalline tips are typically used as thermoionic sources.

3.1.2 Lenses in Electron Microscopes

Although many parallels can be drawn between light and electron optics, electron microscopes require electromagnetic lenses to direct the electron beam as desired. Figure 3.3 shows a schematic cross-section of an electromagnetic lens. Due to the nature of those lenses, a *stronger* lens will result in a less

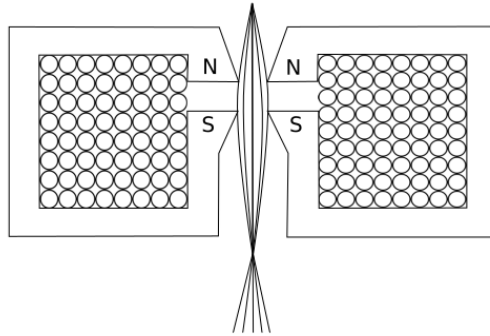


Figure 3.3: Schematic cross-section of an electromagnetic lens. The specimen and objective aperture are located between the upper (N) and lower (S) pole pieces.

magnified image. A lens is called *overfocused* if its strength is increased and the image is formed above the focal plane. It is called *underfocused* if it is weakened and the image is formed below the focal plane [8, p. 96]. The

effect on the position of the image in relation to the focal plane can be seen in fig. 3.4. The operation of an electron microscope that is out of focus can

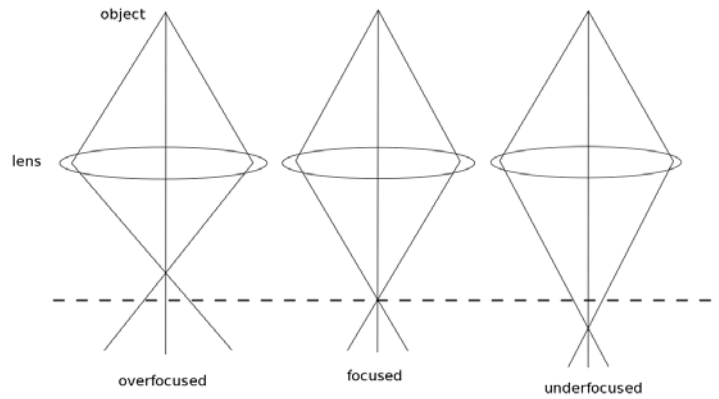


Figure 3.4: Schematic representation of over-, under- and focused lenses. Dashed line is the focal plane.

also lead to the obtainment of valuable information, as is not the case with a visual light microscope. An underfocused lens will offer electron beams that are more parallel to each other and the optical axis, improving image contrast.

3.1.3 Interactions of Electrons with Matter

There are numerous possible interactions that occur between electrons and matter. Not all are equally desirable, and their usefulness depends on the nature of the specimen. It is for instance not very common to use diffraction patterns of biological samples in electron microscopy. As electrons reach the sample, they are scattered, resulting in a range of observable effects, see fig. 3.5. The scattered electrons may be divided into *forward* and *back scattered electrons*, depending on whether the scattering angle lies below or above 90° . For TEM, it is forward scattering that is used in image production. It consists of the direct electron beam, the majority of elastic scattering, diffraction, refraction and inelastic scattering. An electron might be scattered once, i.e. a *single scattering event* occurs, or more than once (this is referred to as *plural scattering* and starting from 20 scattering events for one electron

multiple scattering). In general, scattering processes will be simplified to single scattering events. Another helpful aspect to characterise and explain scattering in TEM is by taking the wave-particle duality of electrons into consideration. Certain mechanisms are better explained using either one or the other aspect of the electron's nature.

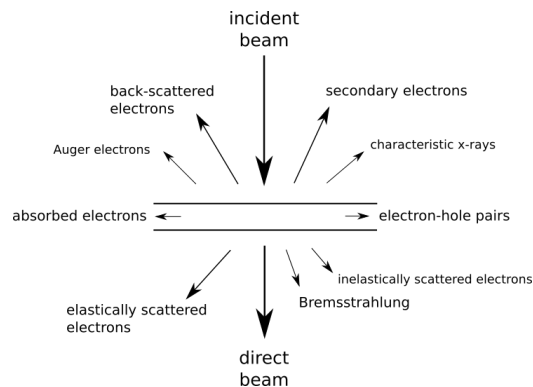


Figure 3.5: Interactions resulting from the impact of the electron beam onto the specimen.

Elastic Scattering

The kinetic energy of the elastically scattered electrons is preserved. As a simplification, electrons with only minimal loss of energy will also be regarded as such. The majority of the contrast in images results from elastically scattered electrons. When interacting with single, isolated atoms, electrons from the beam may interact with either the electron cloud of the atom, or also with the positive nucleus. The latter produces much larger scattering angles, see also fig. 3.6.

Diffraction

Another form of elastic scattering is best explained using the wave nature of electrons. The Huygens-Fresnel principle already describes the behaviour of the wave propagation of visible light. It postulates that each disturbance a wavefront encounters is a source of spherical waves. The electron beam is treated as a wave interacting with a group of atoms in the specimen.

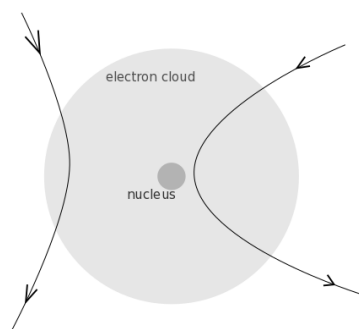


Figure 3.6: Electrons passing close to the nucleus will have a greater scattering angle.

Each atom in the sample will lead to diffraction of the electron beam wave. Scattered waves may interfere with each other, leading to *constructive* or



Figure 3.7: Example for diffraction of a plane wave at a obstacle.

destructive interference. This is characterised by the phase shift and whether the amplitude of the resulting wave is larger or smaller than the individual amplitudes. The resulting diffraction patterns (DP) can be used to determine the crystallographical structure of the sample. DPs are less useful when imaging amorphous samples, which most biological specimens are.

Refraction

Refraction refers to the change in direction of a travelling wave as it enters another medium. The velocity of the wave may change, although the frequency will not. This phenomenon will occur when the wave of the electron beam enters the sample and the medium changes from air (vacuum) to resin and again to air at the exit of the wave.

Inelastic Scattering

Another large component of electron scattering in TEM is inelastic scattering. Methods such as electron energy loss spectroscopy (EELS) use inelastically scattered electrons to obtain valuable insights into the elemental composition of biological samples [9]. An inelastically scattered electron loses energy as it interacts with the specimen. A thicker sample would lead to the occurrence of several scattering events and thus, a greater energy loss.

This may lead to the production of X-rays, either of characteristic or of Bremsstrahlung type. In the case of characteristic X-rays an incoming electron knocks out an electron in an inner shell, which is then replaced by an electron from an outer shell. The descent of the latter causes a release of energy in the form of X-rays. The energies of those X-rays are unique to each type of atom and therefore allow a composition analysis of the sample. Bremsstrahlung X-rays are produced by an incoming electron moving through the sample and interacting with the nucleus/ It then suffers a change in momentum and may emit X-rays (up to beam energy).

Besides the emission of X-rays, inelastic scattering processes can also induce the emission of secondary electrons. Those are electrons that originally are part of the sample, but are ejected from their positions by the incoming beam electron. When secondary electrons are ejected from the conduction or valence band of the atom, they have low energies and do not contain any information of the composition of the sample. However, they are useful for the characterisation of the surface topology, a method used by scanning electron microscopes (SEM). Another type of secondary electrons are Auger electrons. Their production process is similar to the one of characteristic X-rays. As an electron from an outer shell replaces the electron ejected from an inner shell, it transfers energy to an electron also positioned in an outer shell. This electron has a sufficient amount of energy to leave the atom as an Auger electron.

Lastly, inelastic scattering in the specimen is the main cause of beam damage. Ionization of the atoms in the sample by incoming electrons, called *radiolysis* can lead to a break-up of chemical bonds in materials. The incom-

ing electron beam may also displace atoms or even eject them. The latter case is referred to as *sputtering*. Another important type of beam damage is *heating* of the sample. When the atomic lattice is struck by a beam electron, the atoms begin to oscillate collectively, such oscillations being *phonons*. Heating of the specimen depends on many factors, including its thickness and thermal conductivity where a lower thermal conductivity will lead to higher heating. Heating may thus present a substantial problem when imaging biological samples. To counteract this effect, the specimen can be cooled within the microscope using liquid nitrogen (LN₂).

3.1.4 Detection of Electrons

The human eye does not possess the ability to ‘see’ electrons, which is why a scintillator is typically used to convert electron to photons for visualisation on a viewing screen or a camera. The intensity of the light emitted by the scintillator is proportional to the intensity of electrons it receives.

It is common for most TEMs to possess a viewing screen in the lower part of the column. The screen is coated with a material that will fulfill the above requirements, for instance Zinc Sulfide (ZnS) and then doped, changing the wavelength of the emitted light. This leads to the emission of green light, a wavelength at which observation of the screen is most relaxing for the eyes.

Charge-coupled device (CCD) cameras are now mainly used to record images. They are able to detect incoming electrons and thus allow the conversion of previously analog images into digital ones.

3.2 Sample preparation

Biological samples need to be prepared to withstand the vacuum and harsh electron radiation inside an electron microscope before they can be observed. Additionally, to limit inelastic scattering and beam damage, the sample should be very thin (in the order of 100nm). In order to preserve ultra-structural details, careful and extensive preparation is required. One of the most common methods to fixate biological samples is CF. Another, more

technical method, is HPF with subsequent FS. Finally, the sample must be embedded into the right medium, in order to be sectioned, perhaps stained and then imaged.

3.2.1 Chemical fixation

In CF highly reactive chemicals are used to form crosslinks in between proteins or lipids so that the biological sample is “fixed” and does not undergo structural changes and rearrangements during dehydration and resin embedding. The most commonly used fixatives are GA and OsO₄.

Glutaraldehyde

GA (see fig. 3.8) kills cells rapidly by crosslinking proteins on an intra- and intermolecular level upon polymerisation. It is most effective when preserving fine structure and importantly, fixation is irreversible. It can be used for all different types of living organisms but also already deceased ones.

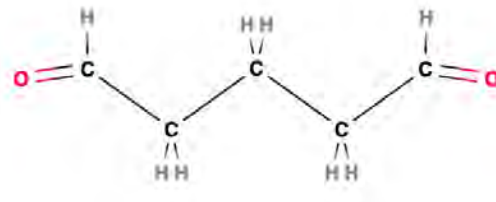


Figure 3.8: Glutaraldehyde molecule. Image from [10].

As a liquid with low viscosity, it is soluble in water and other organic solvents, rendering them slightly more acidic. It is moderately toxic and should therefore be handled with care. This however is not much of an obstacle during sample preparation, especially when comparing to other chemicals and methods of preparation. An advantage of GA is that it does not induce significant changes in protein conformation, although the protein molecule may suffer structural modifications. The effects of GA on various components of cells are listed below, with reference to [11, p. 28-41].

GA preferentially reacts with the amino acid lysine. Others involved include tyrosine, tryptophane, histidine, phenylalanine and cysteine. The exact reactive processes occurring during crosslinking are still debated upon, but Hardy *et al.* have shown that pyridine derivatives are major reaction products [12]. Crosslinking of protein with glutaraldehyde is discussed further in [13].

The impact of GA when interacting with lipids is still uncertain. Preparation of samples for EM affects the phospholipid bilayer in cells and GA may be able to prevent its loss. It is supposed that reactions with phospholipid occur when those have free amino groups, i.e. phosphatidylserine (PS) and phosphatidylethanolamine (PE). PS has strong hydrophobic bonds connecting it to proteins in the membrane, which might be responsible for its preservation. Phosphatidylcholine (PC) and phosphatidylinositol (PI) do not possess primary amines; dehydration and embedding would cause them to be extracted.

Most probably, glutaraldehyde reacts with polyhydroxyl compounds of carbohydrates, leading to the formation of polymers. GA results in the retention of glycogen in the tissue (around 40-65%), which can then be stained using a silver solution.

GA can be used in a range of concentrations without resulting in many detectable differences on the quality of the fixed sample. Regarding osmotic activities of the cellular membrane, the total osmolarity and concentration of the solution containing the fixative is much more significant than solely that of GA. Because the fixative solution requires a certain period of time to act upon the sample, a rise in the osmolarity of the solution may occur. The osmotic property of membranes and other activities involving the cell's metabolism are partially conserved. Therefore adapting the osmolarity of the washing and dehydration solutions can be advantageous. Even after fixation with GA, the cell membrane remains permeable to sucrose. This for example is not the case after treatment with osmium tetroxide.

The extent of reaction to GA is proportional to the temperature at which it is being used. Room temperature (RT) can be preferable as it increases the rate of penetration and fixation. Lower temperatures help to minimise

extraction by delaying the onset of autolysis. It also reduces the shrinkage of mitochondria, granularity of cytoplasm, volume changes and artifacts. Additionally, it is advantageous when fixing extremely labile enzymes. Adequate penetration is hindered by dense tissue, especially at temperatures below RT.

As long as it remains within a sensible range of 1.5% to 4%, the concentration will not affect the quality of the fixation. If the concentration is too high, it leads to excessive shrinkage of cellular components. Additionally this effect does not manifest equally in every part of the cell. A too low concentration of GA causes intense extraction during the washing and dehydration steps because the affected components will not have been properly fixed. Slower penetration does not justify the use of a higher concentration because the increased cell damage outweighs the faster fixation.

Out of all factors influencing the fixation process when using GA, the pH is the most influential. The binding capacity increases with the pH value. A higher pH also drives quicker polymerisation, which in excess may produce artefacts. In [14] the authors advise mixing the GA and buffer only immediately before when using solutions with a pH above 8.5. During fixation the pH of the solution drops, impairing its crosslinking capabilities. The decrease in pH can be reduced by using the appropriate buffer, which can counteract a change in the concentration of positive hydrogen (H) ions.

Because here the rate of penetration can be regarded as equal to the rate of fixation, it is an obvious factor to be considered when evaluating the suitability of a fixative. Above all, it depends on the concentration of GA and the type of specimen being fixed. Other important elements are the previously mentioned pH, temperature and type of buffer. Even with a perfect interplay of all components, the sample size remains limited to a maximum of 0.5mm per dimension. Prolonged fixation does not offer a compensation for low penetration rates. Instead, it can be increased using chemicals, e.g. formaldehyde, as aids.

The main consequence of a fixation with aldehydes that can be observed are dimensional changes of the imaged structures. Due to the osmotic shock taking place during fixation, the specimen is bound to shrink. A reduction

in size of up to 5% in each direction is possible. A higher osmolarity of the fixating solution will result in greater shrinkage. Its severity is dependent on the concentration and type of specimen. Contraction of the extracellular space may be provoked by an increase in permeability to sodium ions of the membrane during fixation. The extent of shrinkage varies within the cell, e.g. it affects the cytoplasm to a different degree. A fixation with GA leads to more shrinkage in the cell's nucleus, but to less in the cytoplasm, than fixation with OsO_4 . Some shrinking effects can be overcome by follow-up treatments. It has also been observed that age plays a role; older cells are more likely to be subjected to dimensional changes than younger ones. Isolated cells also are more affected than those in tissue. Adjusting the osmolarity of the solutions involved helps reduce shrinkage in the specimen. This includes the solutions used for the washing steps and post-osmication.

Although GA is a great fixative, it does not provide contrast for observation using electron microscopy. This lack of contrast enhancement is most obvious at cellular membranes which often appear whitish in EM images. This is caused by certain lipids being insoluble in organic solvents which prevents staining agents in solvents from reaching them. Because it also does not fixate phospholipids well, artefacts may be produced in membranes. GA is also not usable in cold temperatures, which may be a requirement for specific samples. Membrane fluidity is not affected by fixation with GA, it is however entirely eliminated by OsO_4 . Lastly, GA unfortunately does not offer full protection against extraction of components in the later steps.

Osmium Tetroxide

Osmium tetroxide is an effective compound for fixation and staining. It is normally used as postfixative because it leads to the preservation of lipids, despite its inability to crosslink most proteins and preserve carbohydrates. As osmium is a heavy metal it also acts as stain, adding electron density and thus producing high contrast for electron microscopy.



Figure 3.9: Molecule of osmium tetroxide. Image source: [10].

The non-polarity of OsO_4 (structure formula in fig. 3.9) allows it to also penetrate charged surfaces, such as cell membranes, and tissues. It is soluble in water and will keep constant pH if dissolved in double-distilled water (ddH₂O). In a hypotonic aqueous solution it will increase the osmolarity of the final fixating solution. Osmium tetroxide, as well as its vapour, is extremely toxic, and very volatile. It should be handled with extreme precaution under a fumehood and contact with any organic matter must be avoided. Osmium will easily reduce any organic material upon contact and lead to discolouration and darkening. Although a change in colour is not a clear indicator for a reaction, the hue of the solution before usage can be useful for determining its age and quality. Despite slow penetration, OsO_4 offers excellent quality tissue preservation of most samples and is also very effective for use during freeze substitution. [11, p. 45]

Using OsO_4 results in partial retention of lipids, preferentially unsaturated ones. The double bond in unsaturated lipids are the initial and also often primary site for a reaction. Although osmium tetroxide leads to a change in the structural properties of lipoproteins, it does not destroy them. It does however, lead to a change in membrane thickness during fixation. By crosslinking proteins and lipids, it blocks any motion in the lipid bilayer. This causes the membrane to become permeable to small ions and molecules: proteins diffuse out of the cells. The amount of lipids lost during osmication is often underestimated. A large amount is already present and the morphology of the sample does not change by much despite the loss of lipids, some of which are already extracted in the osmium step. Loss can be minimised when using osmium after a glutaraldehyde fixation and with either only partial dehydration or dehydration at 4°C. The degree by which lipids

are extracted from the sample depends on the type of lipids and the type of tissue being fixed.

Certain proteins, such as albumin, globulin and fibrinogen lead to gelling when reacting with weak solutions of osmium tetroxide. The reactions occur at different concentrations and rates depending on the proteins. This may be related to a dependency to the amount of tryptophan which has many double bonds. The pH influences the reaction of OsO_4 with specific amino acids. A higher molecular weight decreases the rate of formation of precipitate. The secondary structure of soluble and also membrane proteins may be altered due to treatment with osmium tetroxide. This can be the cause of extraction of cellular material in the follow-up steps. Most proteins are lost in fixation and dehydration steps. Even succeeding GA fixation, osmication can lead to more severe change in protein conformation. Extraction of proteins and its degree are dependent on many factors, including the duration of fixation and dehydration, and the type of buffer and type of protein. An exceedingly long fixation also causes the destruction of cellular protein.

Because of its slow penetration rate, osmium is not suitable for the preservation of carbohydrates. [11, p. 49-50]

Osmium causes hardening of the tissue and also changes in specimen volume. Osmicated cells typically show swelling coming from the osmolarity of and the type of ion in the fixation vehicle and also the type of specimen being fixed. It is to be noted that tissue after osmication still exhibits a smaller change in volume than without osmium treatment, due to the shrinking effect of dehydration and embedding. Volume changes can be avoided by adjusting the osmolarity of the solution. This can be done by adding CaCl_2 or NaCl ions when using osmium as primary fixative, and either NaCl , glucose or sucrose if it is a secondary fixative. CaCl_2 enables the reduction of the osmotic pressure within the cell, decreasing swelling. NaCl may be the preferential additive for secondary fixation as glucose and sucrose do not prevent the flow of water into the cell.

Concentration of osmium solutions is commonly between 1 and 2% in buffer. If it is too high, it will cause oxidative damage to protein molecules and result in peptide fragments being lost. For certain specimens, a concentration

of as little as 0.2% may prove to be useful.

Instead of fixating samples at RT, it should be done at 4°C. A lower temperature will assure slower autolysis of cells and therefore improve the loss of components by extraction. It also provides a more uniform fixation.

The rate of penetration into the specimen depends on the density of the tissue, concentration of the solution, temperature and also whether fixation is performed by perfusion. Because osmium solutions are made in buffer to regulate osmotic pressure in the sample, penetration is slowed down. The diffusion gradient decreases over time, probably due to the formation of a barrier by the already fixed surface. To achieve reasonable penetration, the tissue size should not exceed 1mm³. [11, p. 57-59]

Recommended duration of fixation lies between 15min and 2h. It is directly related to the temperature, lower temperatures requiring longer fixation times. The optimal length of fixation is dependent on concentration of OsO₄, buffer and varies among specimens. A compromise is necessary to achieve the highest quality of fixation and simultaneously the least possible extraction.

OsO₄ may produce precipitates referred to as osmium blacks. They are amorphous and water-insoluble but have strong electron scattering properties therefore producing high contrast.

Although GA and OsO₄ complement each other well for the fixation of biological samples, their successive use may be unfavourable in some cases. Glutaraldehyde does not modify the fluidity of the lipid bilayer whilst producing crosslinks between proteins. This can cause the formation of aldehyde-induced artefacts which cannot be remedied by the use of OsO₄. A mixture of the two fixatives can produce sharp membranes and improve structural preservation.

Buffer

Fixating media tend to decrease the pH of the solution. The choice of the right buffer appertains to the quality of fixation. Two commonly used buffers are phosphate and cacodylate buffers. The former are good at stabilizing the pH of the solution, and their main advantage is their resemblance to

physiological environments. Care must be taken during the storage to avoid contamination. Precipitations are likely to occur, especially in the presence of uranyl acetate or lead salts (used in post-staining). Those manifest as electron dense spheres in the prepared specimen.

Cacodylate buffers have a pH in the range of 6.4-7.4, but it drops after addition of the fixative [15]. Storage is simplified and the buffer remains effective for a longer period of time as cacodylate buffers do not allow the growth of microorganisms. The formation of precipitates is hardly an occurrence [16], posing an additional advantage of these buffers. However, they lead to change in the permeability of the cell membrane, resulting in a redistribution of cellular material along an osmotic gradient in the cell. Buffer is also used for rinsing the sample between glutaraldehyde fixation and osmication.

Dehydration

As most resins are immiscible with water, it needs to be removed before embedding. The specimen is successively immersed in solvents of increasing concentration. Ethanol may be used, but acts as a coagulant fixative, damaging the specimen. Following ethanol dehydration, a transitional step in propylene oxide is required before resin embedding. Alternatively, acetone qualifies as dehydration agent by showing little reactivity and being miscible with resin. Acetone produces less shrinkage and lipid extraction than ethanol, but cannot be considered an ideal solvent for dehydration in every case. Undesirable side effects of dehydration include shrinkage of 5-70% and extraction, which is why a short duration is preferable. Dehydration at RT additionally leads to an increased loss of lipids, it should therefore be performed at a lower temperature, at which the samples already are after osmication.

3.2.2 HPF-FS

High-pressure freezing is becoming increasingly popular as fixation method. An extremely high pressure hinders the expansion of ice during freezing and

minimises cellular damage. It is followed by freeze substitution, in which solvents replace the water in the cell at low temperatures.

Freezing

Water has an unusual freezing behaviour, its density lowers upon freezing. In the liquid phase, hydrogen bonds are often broken up by the presence of thermal energy. When freezing, the thermal energy is reduced and the hydrogen bonds are less easily broken up [17]. This leads to the formation of a crystal structure by the molecules. Although unusual for a crystalline structure, it is less tightly packed than that of liquid water, leading to an expansion in volume. The majority of tissue mass consists of water, thus being extremely susceptible to freezing damage. During freezing, water molecules agglomerate into a nucleus, providing a starting point for the growth of ice crystals that consequently spread throughout the tissue.

Cellular damage occurs due to a number reasons. Extracellular and intracellular ice formation are responsible for mechanical and structural damage [18]. Expansion of the ice leads to the cells being torn apart or pierced by ice crystals. A change in the concentration of solutes in the remaining liquid phase may also harm the frozen cells [19]. Cryoprotectants are able to influence the total solute concentration, reducing the formation of ice. For the purpose of cryopreservation they must, however, fulfill certain properties such as low toxicity, ability to penetrate the cells and high solubility in water.

Vitrification is an alternative preservation method, avoiding ice crystallisation. Ice nucleation, as well as crystal growth, are temperature dependent. The former reaches a maximum rate as temperature drops, before slowing down due to the liquid's increased viscosity. Ice crystal growth is fastest below the equilibrium freezing point, although at this point the nucleation rate is not at its maximum. It is therefore possible to avoid both nucleation and freezing by using sufficiently rapid cooling rates [20].

High-pressure freezing

A method popular in cryofixation of samples for observation in electron microscopy is high-pressure freezing. Ice nucleation in the sample can be avoided or at least limited, thus minimizing (or even avoiding) damage to the cells. The samples can also be thicker than with other cryofixation methods. A pressure of 2100bar is applied whilst submerging the sample in liquid nitrogen (LN_2). The expansion of water can thus be hindered by applying a high enough amount of pressure. As demonstrated in fig. 3.10, at a pressure of 2050bar the melting point of water is at a minimum of -22°C , and super-cooling may only happen until -90°C [21]. At this pressure, water crystallises as ice II and III. These crystal types are denser than water and also possess lower nucleation and growth rates than ice I, which is formed at lower pressures [22]. Applying those higher pressures, the critical cooling rate can therefore be lowered to -10^{2°C/s for biological specimens whilst still avoiding unfavourable ice crystal formation. This allows freezing of samples that are up to $600\mu\text{m}$ thick [23]. Figure 3.11 shows a typical curve obtained when high-pressure freezing a sample, plotting the temperature and pressure progression over time.

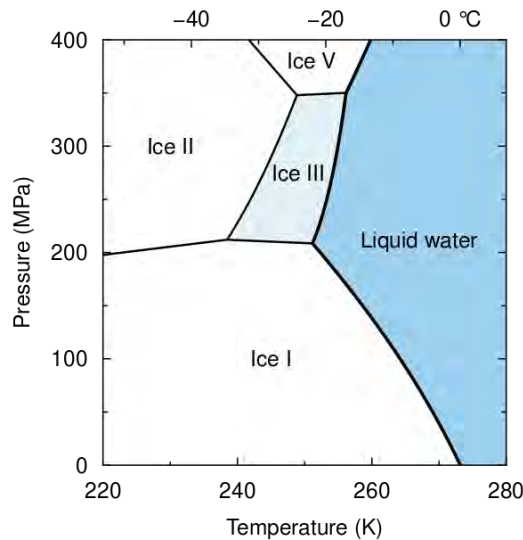


Figure 3.10: Ice phases around the freezing point of water [24]

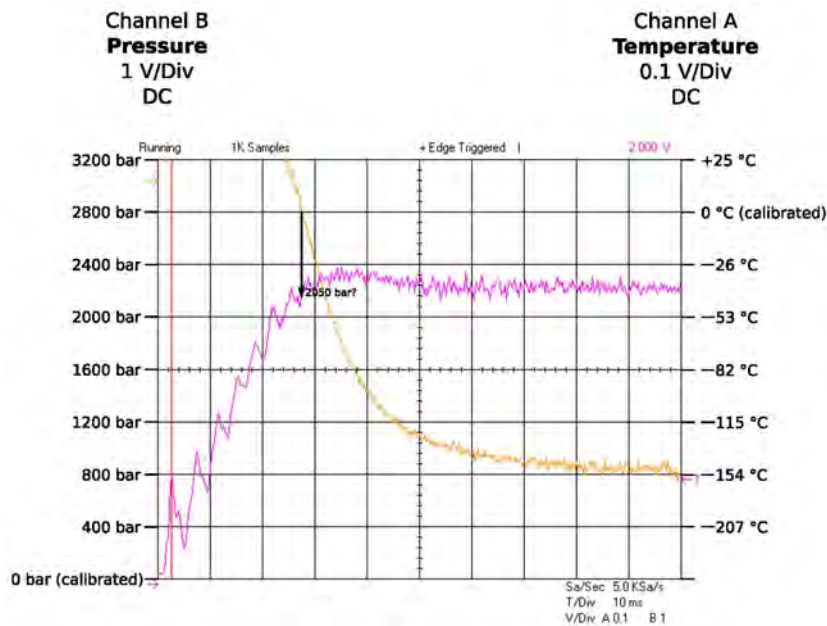


Figure 3.11: Exemplary freezing curve from HPF Compact 01, plotting temperature (yellow) and pressure (purple). Box width 10 ms.

After freezing, the sample is immediately transferred to liquid nitrogen where it can be stored until further handling.

Freeze Substitution

Samples fixed during freeze substitution (FS) are suspected to present less extraction and more accurate preservation as the movement of organelles during FS is restricted. Moreover, FS allows slow and also continuous dehydration of the sample, improving ultrastructural preservation. The idea behind the process is to replace ice in the specimen by a solvent. FS medium in acetone is prepared and distributed amongst vials, pre-cooled to -160°C and the samples deposited on top. Roughly 0.5ml of medium are used per vial. They are first warmed to -90°C , at which point most of the ice is dissolved. The subsequent temperature steps depend on the ingredients of the FS medium. Uranyl acetate works at very low temperatures already, the best temperature for GA lies around -50°C . OsO_4 is most effective at -20°C . Lastly, the samples are warmed to 0°C and rinsed on ice using acetone.

All steps before and after freeze substitution require care. Contact with air and objects of higher temperatures must be avoided. Short warming of the samples could result in a recrystallization of the ice, defying the purpose of high-pressure freezing.

3.2.3 Embedding and Sectioning

The resin used for embedding has a much higher viscosity than the solvents previously used. To ensure complete infiltration it must be done gradually. Mixtures of resin and solvent with a decreasing concentration of the latter are successively used. It is vital that those are well mixed, a separation of the components would induce differences in the rates of penetration. Storage in an exsiccator for a few hours before polymerisation is beneficial as high environmental humidity is detrimental. The here used epoxy resin requires heat polymerisation at 60°C for 48h. Some other types of resin can be polymerised by ultraviolet radiation. Caution is required as excessively long embedding steps promote extraction. Poor embedding is made visible by holes in the final section.

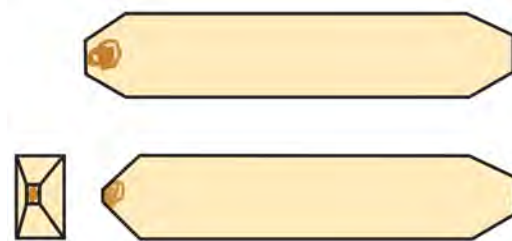


Figure 3.12: Schematic example of an untrimmed resin block (top) and a trimmed block (bottom). The trimmed part of the block will have the shape of a square-based pyramid with its end cut off.

The sample, embedded in a resin block (see fig. 3.12), must be trimmed to a blockface and sectioned to achieve a thickness in the range of 100nm. This is usually done using a microtome and a glass or diamond knife. The block is clamped to a holder, fixed to the microtome and aligned to the edge of the knife. Behind the knife is a basin containing ddH₂O, where the sections

are later collected with a grid. All sections in this work were cut to 70nm thickness. Grids with 100 mesh and covered with a Formvar film were used for collection of sections.

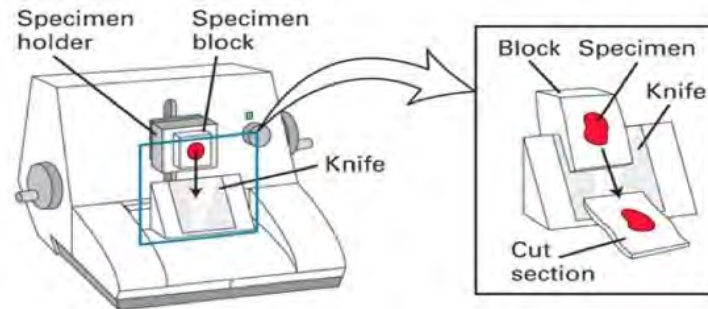


Figure 3.13: Schematic overview of sectioning at a microtome. The specimen block is moved over the knife and the sections slide into a water basin where they are later collected with a grid. Image from [25].

3.2.4 Post-Staining

To increase electron density and improve contrast, samples are post-stained using a positive staining technique. Uranyl acetate and lead citrate are two common staining agents that allow the adsorption of heavy metals to the sample.

Uranyl acetate

Containing the heavy metal uranium, uranyl acetate (UA, shown in fig. 3.14) is extremely efficient at scattering electrons, largely improving contrast of the sample. It is usually used in an aqueous solution of 2-4%. In water, uranyl ions can be found as different complexes. They are able to bind to negatively and positively charged ends of proteins, hence proving UA's effectiveness as stain. It demonstrates a preference for nucleic acids, followed by proteins. Phospholipids are also a favourable target, thus UA is able to influence, penetrate and stain the membrane bilayer. UA reacts easily with cacodylate and phosphate buffers, causing the formation of precipitates. It should be noted that a UA solution will entirely penetrate the section and

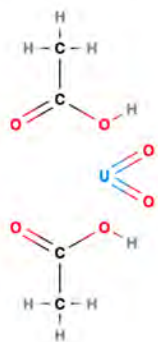


Figure 3.14: Uranyl acetate molecule compound. Source: [10]

stain the sample throughout. It is often used in combination with lead citrate, although it is imperative that the grid is thoroughly rinsed between the two steps. UA is to be handled with utmost care, due to its high toxicity and radioactivity.

Lead citrate

Lead citrate (LC, see also fig. 3.15) is a popular stain used to increase electron density, especially because of its ability to bind to a variety of ultrastructural elements.

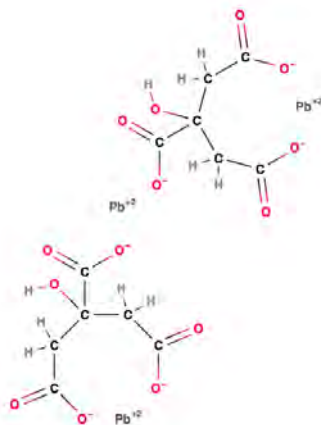


Figure 3.15: Lead citrate molecule. Image from [10]

Staining occurs by the binding of Pb^{2+} ions and its speed increases with the pH of the solution. Membranes are stained if they previously have been processed with OsO_4 . LC also reacts well with glycogen in specimens, and the -SH group of amino acids. Lead salt solutions have a strong tendency to form precipitates in the presence of air, this is lightly reduced in the case of LC by the addition of citrate. Sodium hydroxide pellets are used whilst staining to reduce the formation of lead carbonates which can be observed as highly electron dense amorphous spots on the section. LC is toxic and skin contact should be avoided. Grids should always be rinsed thoroughly but not excessively to avoid washing out with ddH₂O after staining.

3.3 Specimens

Specimens chosen for this work are all of relevance to scientific research and for most part commonly processed at the VBCF EM facility.

3.3.1 *Caernohabditis elegans*

C. elegans is a nematode and very popular model organism in biology. It has a short life cycle and its genome is very compact. Despite its simple anatomy and very limited number of somatic cells (approximately 1000), it is useful for behavioural studies. Most worms are hermaphrodites who self-fertilize and mutants are easy to produce. Important anatomical features that influence preparation for EM include a cuticle on the exterior and partly the interior of the worm. After the embryonic stage, it undergoes four larval stages until it eventually reaches adulthood (see also fig. 3.16). It is easy to cultivate in a laboratory and is fed with *Escheriachia coli* [26, p. 1-6]. Worms cultivated on agar plates in their last larval stage L4 bordering adulthood were used for fixation.

Thank you to Alexander Dammermann¹ and Daniel Serwas¹ for the preparation of *C. elegans*.

¹Alex Dammermann Group, Max F. Perutz Laboratories, Vienna Biocenter (VBC), Dr. Bohr-Gasse 9, 1030 Vienna, Austria.

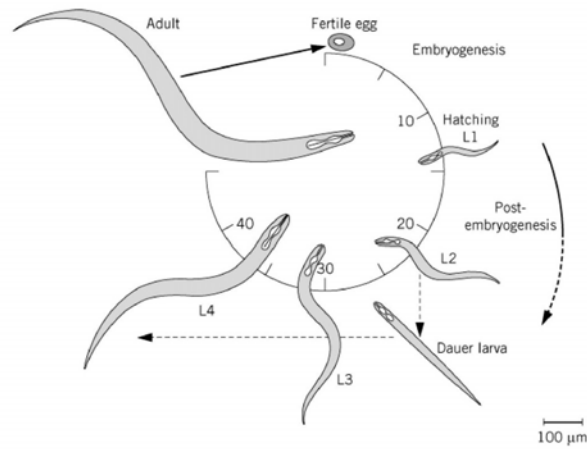


Figure 3.16: Developmental stages of *Caenorhabditis elegans* from egg to adult worm. Image taken from [6].

3.3.2 Cyanobacteria

Cyanobacteria – often mistakenly referred to as blue-green algae – are found in aquatic environments. They are prokaryotes, and photosynthetic, meaning they are able to produce use sunlight as energy source [27]. Cyanobacteria exist in a large variety, between 200-7500 species, of which some are edible and others toxic [28]. Energy production occurs via photosynthesis, enabled by phycobiliproteins (phycobillins), chlorophyll-a and carotenoids [29]. It is suspected that cyanobacteria are the precursor of chloroplasts in eukaryotic cells capable of photosynthesis [30]. A particularity of cyanobacteria is the ability to convert nitrogen into nitrate or ammonia. Thicker-walled cells, called heterocysts, in the bacterium are responsible for the fixation of nitrogen. Those cells have thick walls that are impenetrable to oxygen, creating an anaerobic environment. They are located in the thylakoids, where nitrogenase occurs, which are internal membranes without or with less chlorophyll.

Arthrospira fusiformis

Arthrospira is a filamentous cyanobacterium more commonly known as *Spirulina*, because of its spiral shape, also seen in fig. 3.17. It preferably lives in salt

water with alkaline pH. It is nontoxic and has become a popular nutritional supplement for its high protein content. [31] Spirulina cells are approximately 1-5 μm large, forming filaments that may be up to several millimetres in length.



Figure 3.17: Spiral shape of an *Arthrospira* bacterium seen under the light microscope at magnification of 400x. Scale bar is 10 μm . Image from [32].

Synechococcus leopoliensis

Synechococcus are usually found as individual cells, also found mostly in salt water. They have an oval shape and are between 0.6 and 1.5 μm in size; refer also to fig. 3.18.

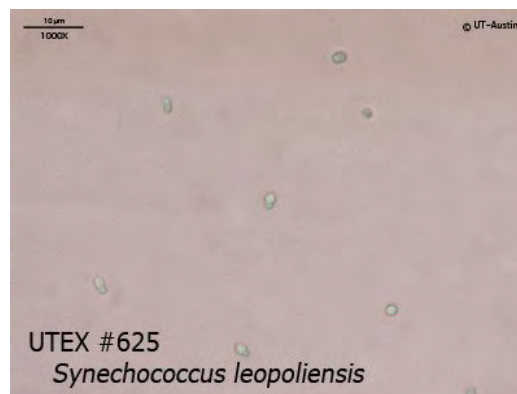


Figure 3.18: *Synechococcus leopoliensis* at 1000x magnification with a scale bar of 10 μm . Image taken from [33].

3.3.3 *Drosophila melanogaster*

Reasons for the popularity of the fruit fly *Drosophila melanogaster* as a research object are numerous. Handling and stock-keeping are easy. The flies feed preferably on rotting fruits as well as yeast cultures, where they also lay their eggs. Its short generation time allows the study of several generations of flies within the span of several weeks. Male and female flies, as well as virgin female flies, are easily distinguishable by the use of a stereo microscope. They possess only four pairs of chromosomes: three autosomes, and one pair of sex chromosomes. The eggs measure approximately 500 μm in length and 180 μm in diameter [34]. The eggs consist of the embryo, enveloped by a very thin vitelline membrane (300nm) and a thicker chorion [35]. The vitelline membrane consists of waxes and is impermeable. The chorion provides mechanical stability and protection, and is also equipped with two dorsal appendages, required for breathing. The formation of an adult *Drosophila melanogaster* takes up to 2 weeks and can be divided into several phases. After embryogenesis, the animal undergoes three larval stages followed by a pupal stage and final metamorphosis into an adult fly. The approximate duration of the individual stages is represented in fig. 3.19.

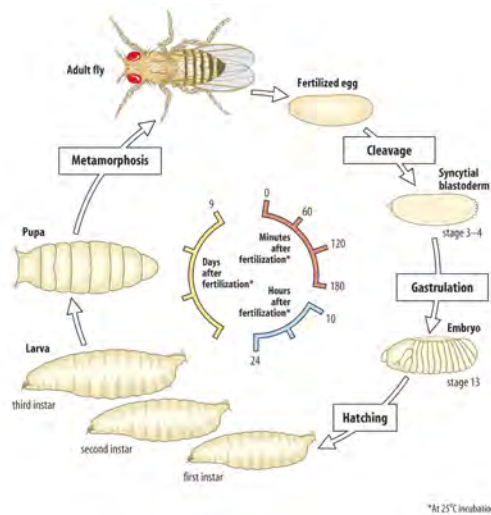


Figure 3.19: Development of *Drosophila melanogaster* from embryo to adult fly [36]

White minus (W^-) flies have a sex-linked mutation on chromosome I,

resulting in white instead of red eyes [37].

Testis

Drosophila testis, the male reproductive organ of *Drosophila melanogaster*, are spiral-shaped. They were dissected from W^- pupae by Jeroen Dobbelaere¹.

Wing Discs

Wing discs are imaginal discs in *Drosophila* larvae that will later develop to wings in the adult fly. They were obtained from third instar larvae of W^- flies by Jeroen Dobbelaere¹.

3.3.4 HeLa cells

In 1951 cells from a cervical tumor were collected from Henrietta Lacks. They have since been cultured in laboratories over the world and are extremely popular organisms for research in molecular biology. They contain the human papilloma virus (HPV), thought to be responsible for the development of cervical cancer. [38] The cells used for this work were cultivated by Harald Kotisch².

3.3.5 NUP60 Yeast cells

Yeast cells can be considered the model eukaryotic cell in biological studies. The most widespread strain used is *Saccharomyces cerevisiae*, also known as Baker's yeast. The cells are approximately of round shape and several micrometres in diameter. In the presently used cells the nucleoporin NUP60 is inactivated, disturbing structural organization in the cell and leading to layered membranes. They were cultured by Anete Romanauska³.

²Facility for Electron Microscopy, Vienna Biocenter Core Facilities (VBCF), Dr. Bohr-Gasse 3, 1030 Vienna, Austria.

³Alwin Köhler Group, Max F. Perutz Laboratories, Vienna Biocenter (VBC), Dr. Bohr-Gasse 9, 1030 Vienna, Austria.

4. Materials and Methods

Every organism analysed was chemically fixed and high-pressure frozen in parallel using the best available protocol. All freezing was carried out using the Wohlwend HPF Compact 1, Engineering Office M. Wohlwend GmbH Sennwald Switzerland, with 3mm Aluminium carriers of different cavities. Freeze substitution was performed in a Leica AFS 2, Leica Microsystems, Vienna, Austria. Embedding steps in resin diluted with a solvent were effected on a rotator or shaker. All samples were embedded in epoxy resin, and polymerised 48h at 60°C. Resin blocks were trimmed using a Leica EM Trim and sections produced using a Leica Ultracut UCT microtome. Imaging was done using the transmission electron microscope FEI Morgagni 268, FEI Eindhoven, The Netherlands, operated at 80 kV, equipped with a Tungsten filament. The images were recorded using a Morada 11-megapixel CCD camera, Olympus-SIS, Münster, Germany.

4.1 *Caernohabditis elegans*

Both protocols used are either taken directly from [6] or are heavily based on them. Stage L4 worms were collected from an agar plate covered in *E. coli* paste using a worm picker.

4.1.1 Chemical Fixation

The 1x cytoskeleton buffer (CB, [39]) was prepared immediately before use from 10xCB and ddH₂O. Chemical fixation proceeded according to the following protocol.

- Transfer worms into vial containing 2.5% GA in 1xCB.
- Cool to and store at 4°C overnight. From this step forth, the worms are kept at this temperature, until embedding begins.
- Centrifuge at 1500g for 30s to pellet the worms at the bottom and facilitate medium exchange.
- Rinse three times in 1xCB for 10min each and pellet again as previously.
- Remove buffer and add a solution consisting of 0.5% OsO₄ in 1xCB for approximately 30min.
- Wash in buffer as before.
- Rinse in ddH₂O for 10min.
- Dehydration for 15min per step in acetone with the following concentrations: 40%, 60%, 80%, 95%, 100%, 100% and 100%.
- First embedding step in a 1:2 mixture of epoxy resin and acetone overnight at room temperature.
- Second step in 1:1 solution for 6 to 8h.
- Third embedding step in 2:1 again overnight.
- Transfer worms into pure resin and store in exsiccator for 6h.

A darkening of the worms will be observable after OsO₄ treatment. The weight of the specimens will increase during osmication, causing them to fall to the bottom of the vial. Thus, the use of the centrifuge with vials containing OsO₄ can be avoided.

In the case of *C. elegans*, the specimens must be pre-embedded in fresh resin within a trough in a small teflon plate and covered with thin aclar film. They are polymerised at 60°C for 48h. After solidification of the resin, the aclar film is removed and the worms cut out using a razor blade. Larger molds are filled with resin and the pre-embedded worms inserted and oriented with

their heads pointing towards the edge of the block. The resin was polymerised again for 48h at 60°C. After hardening and trimming, serial sections of 70nm thickness were cut, and collected on grids. Post-staining was performed with UA for 10min and LC for 5min after thorough rinsing. The main fixation steps are listed in table 4.1.

Step	Reagents	Duration
Chemical fixation	2.5% GA in 1xCB	overnight
Osmication	0.5% OsO ₄ in 1xCB	30min
Dehydration	Acetone in various concentrations	1h 45min
Embedding	Epoxy resin in acetone	2 days
Polymerisation	Epoxy resin	48 h
Post-staining	UA and LC	15min

Table 4.1: Main steps of chemical fixation for *Caernohabditis elegans*.

4.1.2 HPF-FS

For high-pressure freezing, bovine serum albumin (BSA) in a stock solution of 20% in Sørensen buffer was diluted to a final concentration of 5% with M9 buffer. The carrier of 100µm depth was slightly over-filled with cryoprotectant and 5-10 worms deposited within. It was covered with the flat surface of another carrier, inserted in the specimen holder and high-pressure frozen at 2100bar and liquid nitrogen temperatures.

The freeze-substitution medium consisted of 0.5% GA, 2% OsO₄ and 0.25% UA in anhydrous acetone. Table 4.2 shows the temperature (T) course during freeze substitution.

Initial Temperature	Final Temperature	Duration [h]
-140	-90	3
-90	-90	61
-90	-30	20
-30	-30	12
-30	0	15
0	0	3

Table 4.2: AFS protocol for *Caernohabditis elegans*, based on [6].

After the last step, the samples were kept on ice during three 15min washing steps with acetone. The embedding steps were the same as for the chemical fixation, worms were removed from the carriers and embedded in resin molds individually. Sectioning and post-staining were performed in the same manner as for CF.

4.2 Cyanobacteria

Both strains of cyanobacteria, *Arthrospira fusiformis* and *Synechococcus leopoliensis*, were treated using the same reagents and methods. *Arthrospira* were grown and kept in Zarrouk buffer at room temperature, *Synechococcus* in BG-11 buffer, also at RT.

4.2.1 Chemical Fixation

Stock cacodylate buffer was diluted from 0.2M to 0.1M immediately before use. The protocol was as follows:

- Remove bacteria from growth medium and immediately immerse in a solution of 2.5% GA in 0.1M cacodylate buffer.
- Centrifuge at 1400g for 30s and wash three times with buffer for 10min per step.
- Remove buffer and add 1% OsO₄ in buffer and place on ice for 1h.
- Wash thoroughly in buffer and keep on ice.
- Dehydration in acetone for 10min per step at the following concentrations: 40%, 60%, 80%, 95%, 95%, 100%, 100% and 100%.
- The embedding steps (1:2, 1:1 and 2:1 resin to acetone) lasted one night/day each.
- Store in pure resin in an exsiccator for 6h.

The cyanobacteria did not change colour in osmium despite being effectively fixed, as was later observed. They were placed in fresh resin before polymerisation. Solid blocks were trimmed and sectioned to 70nm thickness, placed on grids and post-stained. A summary of the chemical fixation can be found table 4.3.

Step	Reagents	Duration
Chemical fixation	2.5% GA in cacodylate buffer	1h
Osmication	1% OsO ₄ in cacodylate buffer	1h
Dehydration	Acetone in various concentrations	1h 30min
Embedding	Epoxy resin in acetone	2 days
Polymerisation	Epoxy resin	48 h
Post-staining	UA and LC	15min

Table 4.3: Main steps of chemical fixation for cyanobacteria *Arthrospira fusiformis* and *Synechococcus leopoliensis*.

4.2.2 HPF-FS

The filler for freezing consisted of a solution of 5% BSA in Sørensen buffer. Carriers with a cavity of 100µm were used and filled with a few microlitres of cryoprotectant and subsequently with bacteria. To close the sandwich, a carrier with a flat surface was chosen.

FS medium was made up of acetone containing 2% OsO₄ and 0.2% UA dissolved in ddH₂O, resulting in an end concentration of 5% ddH₂O. The protocol is listed in table 4.4.

Upon ending of the freeze substitution, specimens were washed in anhydrous acetone three times for 15min each. Refer to section 4.2.1 for embedding steps. The carriers were embedded in upright standing molds with the sample facing upward. Before trimming, the carriers were broached using a milling machine with a tungsten attachment and leveraged out with a razor blade. Remaining chippings from the aluminium carriers were blown off with high-pressured air and the sample trimmed and sectioned as usual using a diamond attachment or knife.

Initial Temperature	Final Temperature	Duration [h]
-140	-90	0*
-90	-90	40
-90	-54	18
-54	-54	8
-54	-24	10
-24	0	12
0	0	5

Table 4.4: AFS protocol for cyanobacteria *Arthrospira fusiformis* and *Synechococcus leopoliensis*. (*Note: a duration of 0h refers to the minimal amount of time that can be set, as to achieve the maximal temperature gradient when warming the sample from -140°C to -90°C.)

4.3 *Drosophila* testis and wingdiscs

The respective parts were fixed immediately after dissection. In the last dissecting step, they were floating in phosphate buffered saline (PBS).

4.3.1 Chemical Fixation

- Place nets in a multi-well dish and fill with the fixating solution composed of 2.5% GA in 0.1M phosphate buffer.
- Add testis and wingdiscs in separate nets and leave in overnight.
- Wash using 0.1M phosphate buffer.
- Osmication in 2% OsO₄ in ddH₂O for 40min.
- Wash twice in ddH₂O for 10min.
- Dehydrate in acetone at concentrations of 40%, 60%, 85%, 90%, 90%, 100%, 100% and 100% for 10min respectively.
- The first two embedding steps at 1 : 2 and 1 : 1 resin to acetone lasts 2h each.
- The 2 : 1 step lasts overnight.

- Store in molds filled with pure resin in an exsiccator for several hours.

Once in fresh resin, the samples were oriented and polymerised. Flat-embedding holders were used for trimming and sectioning to achieve the correct angle. Figure 4.1 shows the plane at which the specimens were cut.



Figure 4.1: Cutting plane for *Drosophila* wingdiscs (left) and testis (right).

Step	Reagents	Duration
Chemical fixation	2.5% GA in 0.1M phosphate buffer	overnight
Osmication	2% OsO ₄ in ddH ₂ O	40min
Dehydration	Acetone in various concentrations	1h 10min
Embedding	Epoxy resin in acetone	1 day
Polymerisation	Epoxy resin	48 h
Post-staining	UA and LC	15min

Table 4.5: Main steps of chemical fixation for *Drosophila melanogaster* parts.

4.3.2 HPF-FS

Testis and wingdiscs were placed into a drop of 20% BSA in PBS and then transferred to 100µm carriers and covered. The FS protocol is shown below in table 4.6 and the freeze substitution medium being used consisted of 0.1% UA previously dissolved in MeOH and 1% OsO₄ in acetone.

The embedding steps were the same as for chemical fixation. The carriers were embedded in upright standing molds and removed before trimming, refer also to section 4.2.2.

Initial Temperature	Final Temperature	Duration [h]
-140	-90	0*
-90	-90	40
-90	-54	18
-54	-54	8
-54	-24	10
-24	0	12
0	0	5

Table 4.6: AFS protocol for *Drosophila melanogaster* wingdiscs and testis. (*Note: a duration of 0h refers to the minimal amount of time that can be set, as to achieve the maximal temperature gradient when warming the sample from -140°C to -90°C.)

4.4 HeLa cells

The cells were attached to aclar discs covered in fibronectin.

4.4.1 Chemical Fixation

Stock cacodylate buffer was diluted from 0.2M to 0.1M immediately before use. Fixation was done in a teflon dish with circular wells. The protocol was as follows:

- Immerse in a solution of 2.5% GA in 0.1M cacodylate buffer.
- Wash in buffer for 10min.
- Remove buffer and add 1% OsO₄ in buffer for 1h.
- Wash thoroughly in buffer.
- Dehydration in acetone for 10min per step at the following concentrations: 40%, 60%, 80%, 95%, 95%, 100%, 100% and 100%.
- The embedding steps (1:2, 1:1 and 2:1 resin to acetone) lasted 2h each.

For the last step, the discs remained in pure resin for 2h whilst stored in an exsiccator. For embedding, the discs were laid into the lid of a 1.5ml

Eppendorf vial with the cells facing upward. The lid was covered by the vial with its end cut off and filled with resin to obtain a disc a few mm in height. Polymerisation lasted 48h at 60°C. The aclar film could later be peeled from the resin discs. The discs were sawed into four pieces and the individual pieces glued onto previously manufactured cylindrical resin blocks. This way, the samples were sectioned parallel to the substrate. Table 4.7 highlights the most important steps of chemical fixation.

Step	Reagents	Duration
Chemical fixation	2.5% GA in cacodylate buffer	1h
Osmication	1% OsO ₄ in cacodylate buffer	1h
Dehydration	Acetone in various concentrations	40min
Embedding	Epoxy resin in acetone	6h
Polymerisation	Epoxy resin	48 h
Post-staining	UA and LC	15min

Table 4.7: Main steps of chemical fixation of HeLa cells.

4.4.2 HPF-FS

As with *Drosophila* cells, the HeLa cells were adhered to sapphire discs. They were placed atop of 50 µm carriers filled with 5% BSA in 0.1M Sörensen buffer with the cell-side facing down and covered with a polished flat carrier. The freeze substitution medium consisted of 0.25% GA, 0.1% UA and 1% OsO₄ in acetone.

Initial Temperature	Final Temperature	Duration [h]
-140	-90	0*
-90	-90	40
-90	-54	18
-54	-54	8
-54	-24	10
-24	0	12
0	0	5

Table 4.8: AFS protocol for HeLa cells.

Before trimming, the sapphire discs must be broken off. This is done by

trimming the resin around it using a razor blade and submerging the sample in LN₂ several times for a few seconds then leveraging the disc off the resin block.

4.5 NUP60 Yeast cells

The cells were delivered suspended in buffer.

4.5.1 Chemical Fixation

Stock cacodylate buffer was diluted from 0.2M to 0.1M immediately before use. This was the protocol:

- Pellet at 360g for 2min and remove supernatant fluid.
- Wash in 0.1M cacodylate buffer, creating a suspension.
- Pellet as above.
- Add 2.5% GA in 0.1M cacodylate buffer, re-suspend and let sit for one hour. The falcon tube should occasionally be shaken.
- Centrifuge at 360g for 1min.
- Wash the cells in buffer three times buffer.
- Centrifuge at 360g for 2min.
- Remove buffer and add 0.5% OsO₄ in 0.1M cacodylate buffer.
- Set on ice at 4°C and leave for 30min.
- Split the yeast pellets into smaller vials with 0.5ml capacity.
- Wash again with buffer three times.
- Leave in the fridge at 4°C overnight.
- Wash with ddH₂O four times.

- Dehydration for 10min per step in 40%, 60%, 80%, 95%, 95%, 100% and 100% acetone.
- Embedding steps lasted a night/day each and were done at respective concentrations of 1 : 2, 1 : 1 and 2 : 1 of resin to acetone and lastly pure epoxy resin.

If necessary, the specimens can be pelleted between steps for 5s using the short spin programm on the centrifuge. It is however recommended to omit this in steps involving OsO_4 . The yeast pellets were embedded in their vials and polymerised at 60°C for 48h. Table 4.9 gives an overview of CF process of NUP60 yeast cells.

Step	Reagents	Duration
Chemical fixation	2.5% GA in cacodylate buffer	1h
Osmication	0.5% OsO_4 in cacodylate buffer	30min
Dehydration	Acetone in various concentrations	1h 10min
Embedding	Epoxy resin in acetone	2 days
Polymerisation	Epoxy resin	48 h
Post-staining	UA and LC	15min

Table 4.9: Main steps of chemical fixation of NUP60 yeast cells.

4.5.2 HPF-FS

The cells were pelleted at 360g for 2min. Carriers 100 μm deep were filled with 5% BSA in phosphate buffer and small pellets deposited within. The FS medium consisted of 0.2% UA from a stock solution of 2% UA in ddH₂O and 2% OsO_4 in acetone. The temperature steps are listed in table 4.10.

Initial Temperature	Final Temperature	Duration [h]
-140	-90	0*
-90	-90	40
-90	-54	18
-54	-54	8
-54	-24	10
-24	0	12
0	0	5

Table 4.10: NUP60 yeast cells AFS protocol.

5. Results

5.1 Comparison

Following are the results from a comparison of two different fixation methods – CF versus HPF. For both methods, overview images were taken at smaller magnifications as well as close ups at higher magnification. They are compared side by side to determine differences in ultrastructural preservation.

5.1.1 *Caernohabditis elegans*

Figure 5.1 below shows an overview of a transversal cross-section of the nematode *C. elegans*. In the centre is the pharynx of the worm. *Escheriachia coli* bacteria can be seen in the oral cavity and the digestive organ. Around the mouth are smooth muscle cells oriented parallel to the image plane. Various structural elements such as different types of muscle fibers and the external cuticle, can be seen around the above mentioned cells. Close to the worm's cuticle are striated muscles cells, with orientation normal to the image plane, and also mitochondria.

The chemically fixed worm (fig. 5.1, left) generally has a stronger staining, much higher overall electron density, recognisable by its darker colour. This causes lower contrast, diminishing the possibility of distinguishing structural details sufficiently well. Generally, the cuticle and other ultrastructural elements are well fixed throughout the sample. Synapses were preserved excellently. Around the mouth, lighter areas can be observed at the border to the surrounding tissue. The sections had ripped at these precise locations, indicating incomplete infiltration of resin.

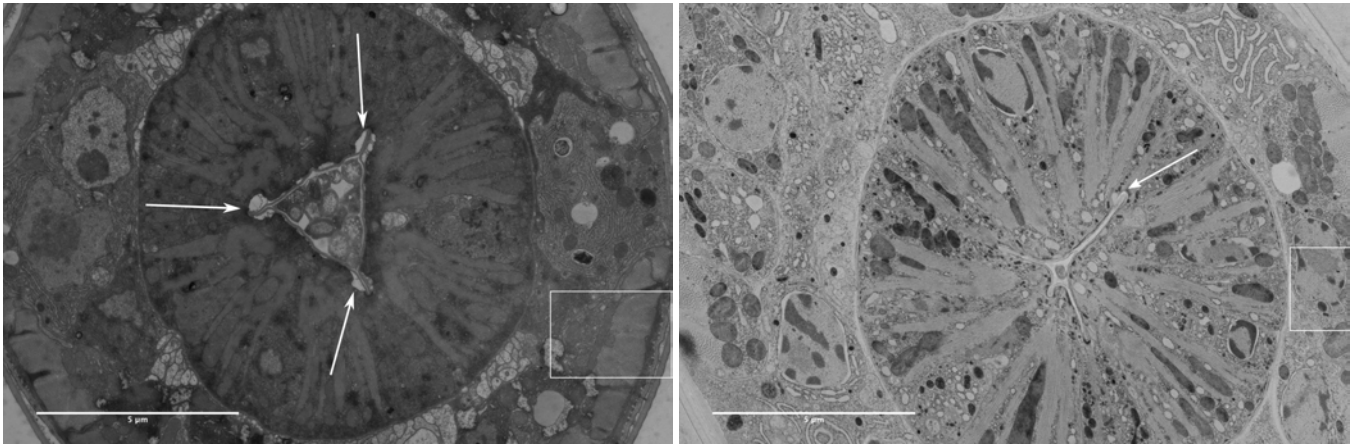


Figure 5.1: *Caenorhabditis elegans* at 7100x magnification, chemically fixed on the left and high-pressure frozen and freeze-substituted on the right. Arrows point out faulty resin embedding. The rectangular areas are the approximate location of the images in fig. 5.2. Scale bar corresponds to 5 μ m.

The high-pressure frozen worm (fig. 5.1, right) overall has a better spread of the staining, a lower average electron density and better contrast. The smooth muscle cells around the buccal cavity are much better preserved, and individual muscle fibres can be made out. Striated muscles cells on the far right and left of the image can be seen very clearly and mitochondria are well defined. The membranes around the smooth muscles and the cuticle show very little contrast compared to the CF specimen. However, embedding is of much higher quality, the worms were thoroughly infiltrated and the resin shows only one small gash. This is also pointed out the by the arrows in fig. 5.1.

Figure 5.2 shows an excerpt of both images, again the CF on the left and HPF-FS specimen on the right. Individual muscle filaments are clearly defined in both images, although the HPF image shows more extraction. The CF image shows more detail and also a denser population of muscle filaments. This may indicate swelling of the specimen after freezing and freeze-substitution. Despite missing contrast, the cuticle in the right image is much smoother and in fact reveals its layered structure. The cytoplasm is much more granular after CF than HPF. Lastly, the greatest difference regarding cell components can be seen in mitochondria. In chemically fixed samples they are swollen and their outer membrane partly separated and

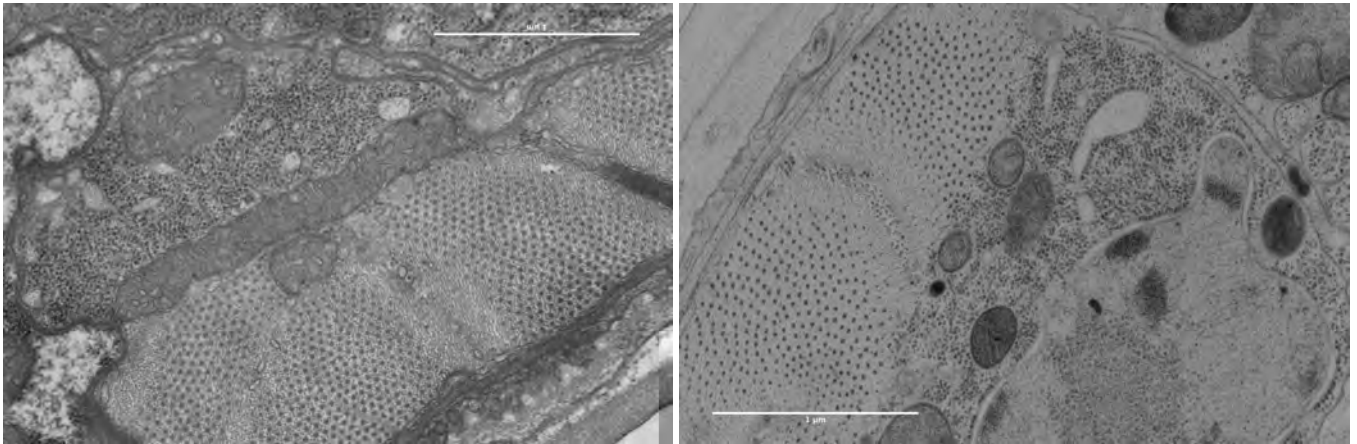


Figure 5.2: Perpendicularly sectioned muscle strands of *Caenorhabditis elegans* anatomy at 36 000x magnification, chemically fixed on the left and high-pressure frozen and freeze-substituted on the right. Scale bar corresponds to 1 μ m.

undulated. Mitochondria aggregate together to form a longer cylindrical one, this is not the case in HPF samples.

5.1.2 Cyanobacteria

Filamentous *Arthrospira fusiformis* are shown in fig. 5.3. Several cells are connected to each other, separated by their respective cell walls. As in section 5.1.1, chemically fixed bacteria have higher electron density, and less contrast.

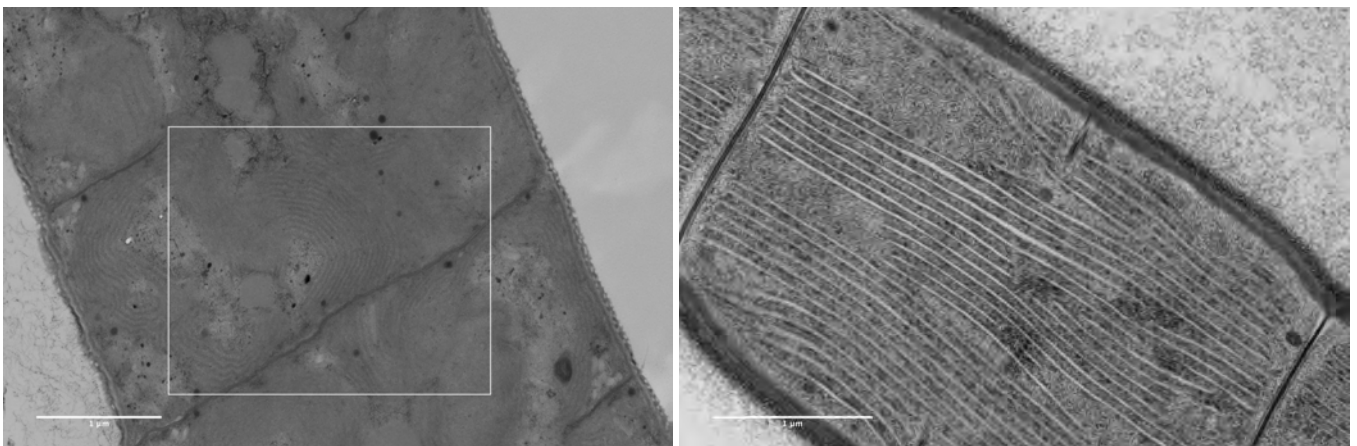


Figure 5.3: *Arthrospira* cells fixed chemically (left, magnification of 22 000x) and using HPF-FS (right, magnification of 28 000x). The bordered area is seen in the left image of fig. 5.4. The scale bar is 1 μ m long.

Chemically fixed samples exhibited undulations in the cell walls, those bordering to the exterior of the cell being the least preserved. The inner and outer cell walls are partially separated after CF. Some holes from improper resin infiltration are pointed out in fig. 5.3. Some arrows indicate dark spheres which can be interpreted as precipitates likely to stem from osmication or lipid droplets. One structure in the CF specimen is most likely a cyanophycin (a polymer responsible for storage of Nitrogen) which is preserved with little detail. Additionally one of the cell walls is breached. It is however unclear whether this is a result of fixation or of cyanobacterial fission, occurring during reproduction. The latter would explain an accumulation of DNA and carboxysomes in the centre of the cell.

On the image of the HPF sample on the right, the cell walls delimiting cells are better preserved. Several layers can be distinguished from one another and they remain smooth. Exterior cell walls, albeit being smoother, are granular and do not reveal much detail. Thylakoids are much more recognisable in the frozen sample, and the space within much larger. This may be an indication of swelling. Lipid droplets are more clearly identifiable as such and DNA filaments. Ribosomes surrounding them are recognisable, but not distinctively delineated.

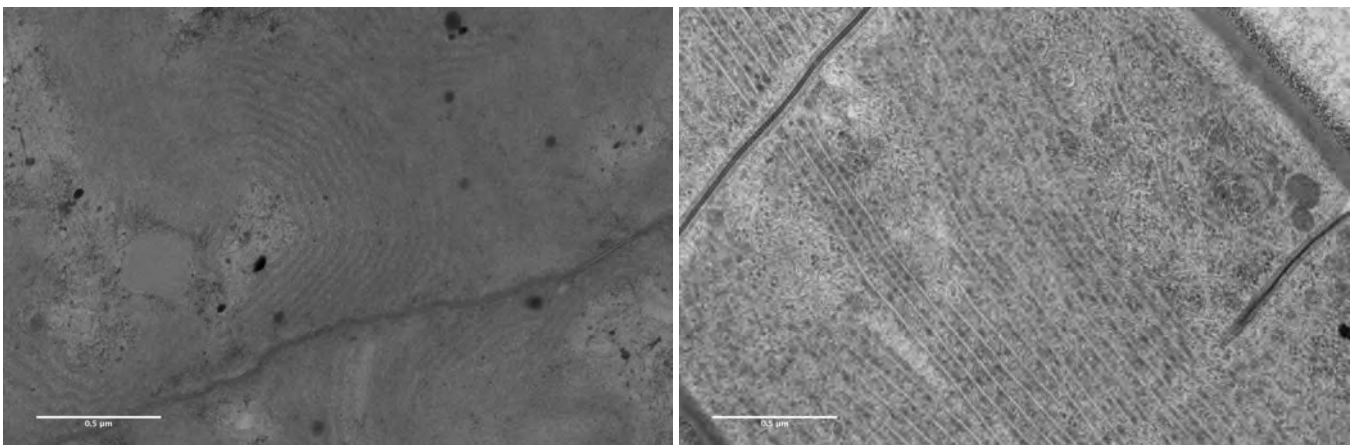


Figure 5.4: Close-up at magnification of 44 000x of cyanobacterial cells. CF on left side and HPF-FS on right side. The latter is taken from the same sample is represented in fig. 5.3 but further to the left of the image. Scale bar is 0.5 μ m.

Figure 5.4 shows cell walls at higher magnification. It becomes obvious the

cell walls in the high-pressure frozen sample are much better preserved. Lipid droplets are clearly delimited, with the appearance of internal structure. DNA filaments can be pointed out as well as ribosomes.

5.1.3 *Drosophila melanogaster* – Testis

Cross sections of *Drosophila* testes are shown in fig. 5.5. This part of the testis contains spermatocyte cysts. The most prominent feature is the flagellum.

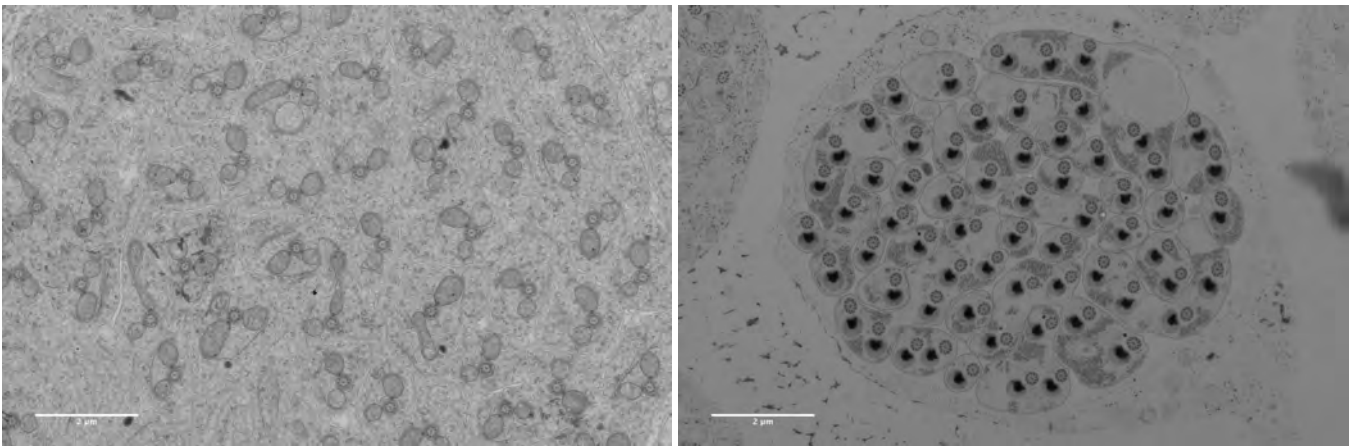


Figure 5.5: Cysts containing spermatocytes in *Drosophila* testis at 8900x magnification. Left shows chemically fixed and right high-pressure frozen. Scale bar is 2µm.

The left image of fig. 5.5 is much less contrasted than the right. Cells in CF testis are closer together. Although the membranes are clearly defined, they appear bumpy compared those in the HPF sample. Much more of the cytoplasm is visible in CF cells, as HPF cells look as if they had suffered from extraction. The latter however display clear membranes, ribosomes and delimited centrioles. Surrounding the cyst, freeze damage is observable.

Figure 5.6 allows a closer look at the spermatocytes. In the right image, the nucleolus is delimited from the rest of the nucleus. Membranes are sharper and smoother than the chemically fixed counterparts. Although centrioles and ribosomes are easy to distinguish, extraction of cellular material is obvious in the frozen samples.

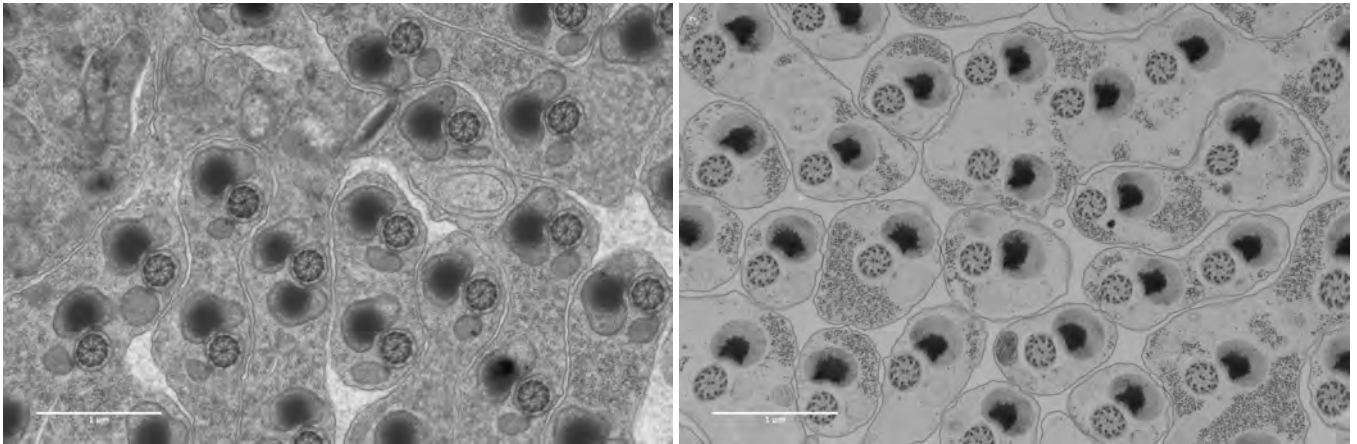


Figure 5.6: Spermatocytes in different stages of development with different fixations: CF, left and HPF, right. At 22 000x magnification. Scale bar: 1 μ m.

5.1.4 *Drosophila melanogaster* – Wingdiscs

Figure 5.7 and 5.8 show cells from the *Drosophila* wing discs.

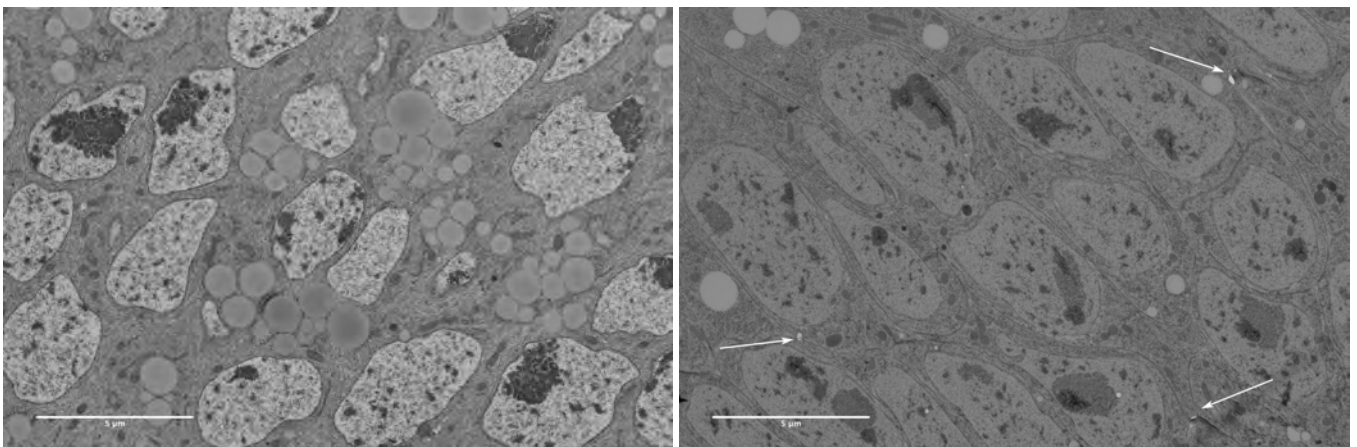


Figure 5.7: Cells in *Drosophila* wingdiscs of L3 larvae at 5600x magnification. CF on left side and HPF-FS on right side. Scale bar of 5 μ m.

The CF specimen, left in fig. 5.8, has better contrast, but also a higher density in large circular spots. Those are either superimposed artefacts of the sample, or uninfiltreated vacuoles. The frozen sample contains small holes, presumably due to faults in embedding. A streak going from the left to the top side of the image also indicates embedding and sectioning difficulties.

Nevertheless, mitochondria and membranes are more clearly delimited and less granularity is present after high-pressure freezing and freeze substitution.

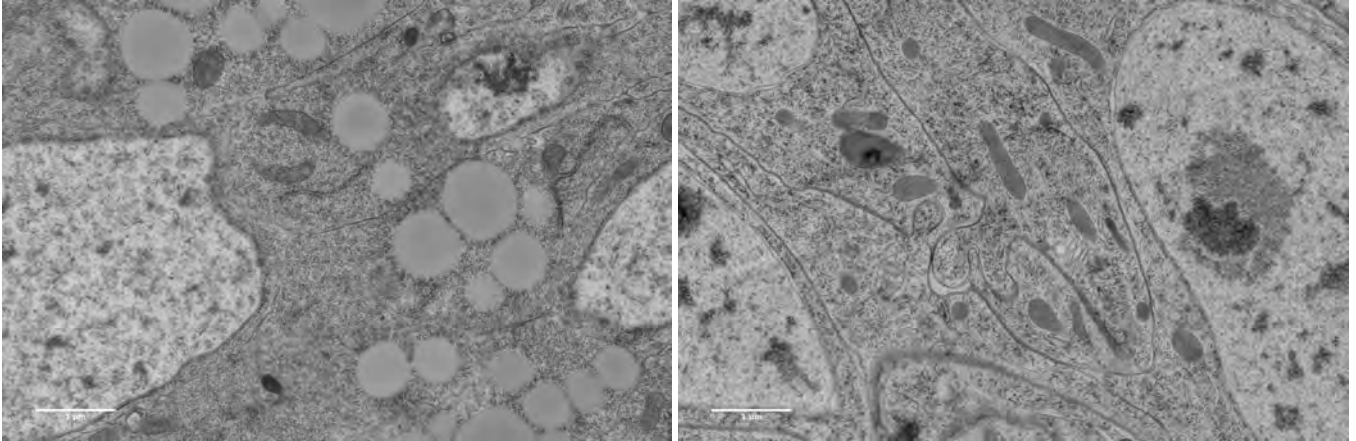


Figure 5.8: Ultrastructural elements of *Drosophila* wingdiscs fixed with CF (left) and HPF (right). Magnification of 14 000x and scale bar of 1 μ m.

A more detailed image (see fig. 5.8) shows that in CF samples the lipid bilayer is often reduced to a single layer. The right image of the aforementioned figure closes in on the streak which is likely to have been caused by a knife mark.

5.1.5 HeLa Cells

Figure 5.9 shows a chemically fixed HeLa cell on the left hand side, and one prepared using HPF on the right. Besides the nucleus, various other cell components such as mitochondria can be observed. Additionally, the cells contain viral inclusions.

Besides a difference in contrast between the two images, the left one also contains traces of debris. It is likely caused by post-staining precipitates. The image on the left does not show a nucleolus and generally appears slightly more extracted than the other. However the CF membrane has smoother appearance than the HPF one. On the right image, mitochondria are very noticeable and virus inclusions easily identifiable.

One of the most obvious differences between the images in fig. 5.10 are the viruses. They are easily located in the HPF sample, where they are even

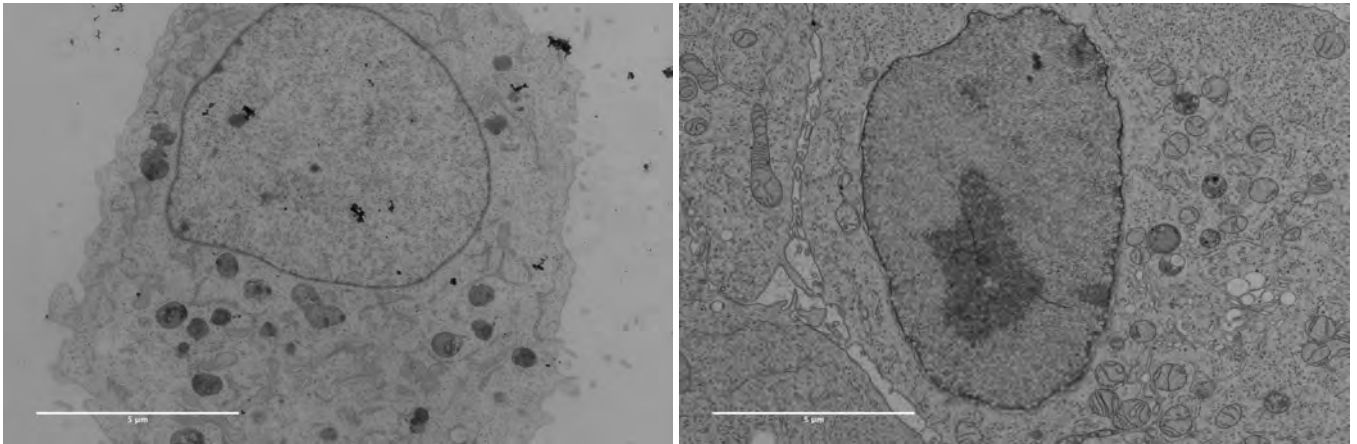


Figure 5.9: HeLa cell at 7100x magnification. Chemical fixation on left and HPF-FS on right. Scale bar of 5µm.

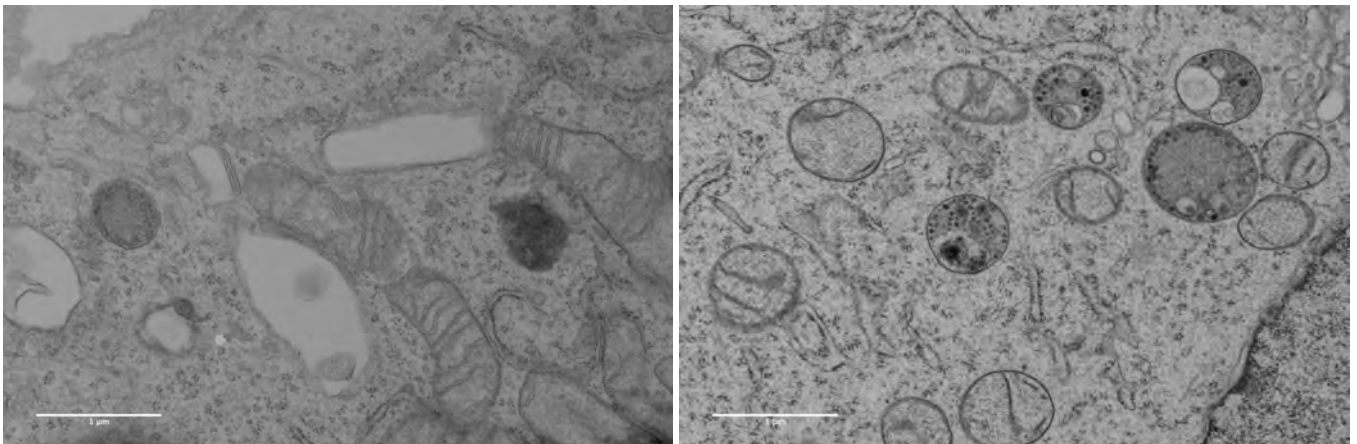


Figure 5.10: Mitochondria and viral inclusions in HeLa cell at 22 000x magnification. Left, chemically fixed; right, high-pressure frozen. Scale bar is 1µm.

countable, but not so in the CF one. In the left image, membranes generally look swollen and as if their layers had separated. This is especially noticeable for the cristae of the mitochondria. The membranes of the inclusions also have suffered from CF. The left image also displays larger "empty" spaces. Ribosomes are equally visible in both specimens.

5.1.6 NUP60 Yeast Cells

Figure 5.11 shows single *Saccharomyces cerevisiae* NUP60 cells.

It is obvious that the chemically fixed cell has an electron density much

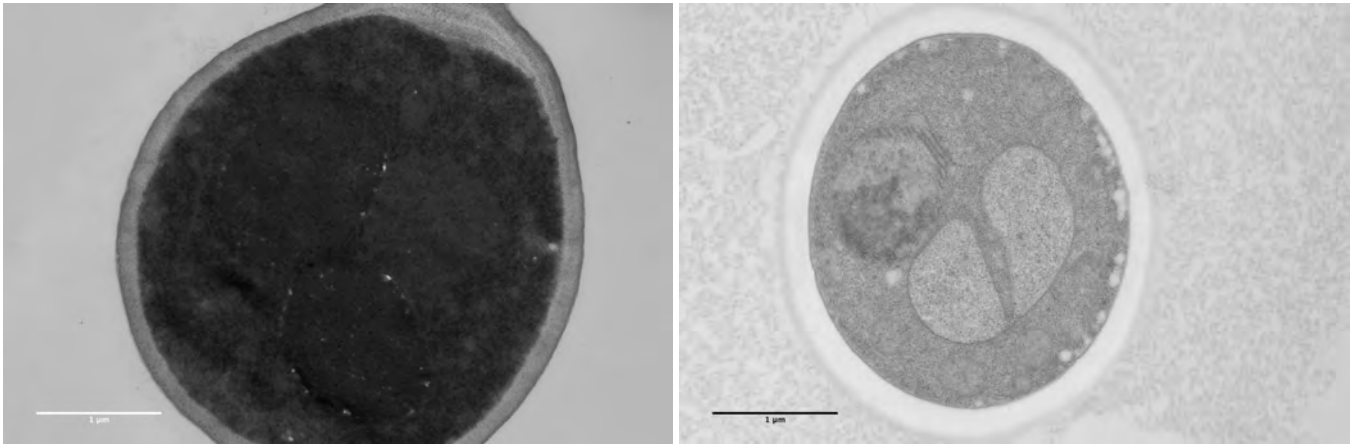


Figure 5.11: Single NUP60 *Saccharomyces cerevisiae* yeast cell, chemically fixed (left) and high-pressure frozen (right) viewed with a magnification 22 000x. Scale bar represents 1µm.

too high to reveal any information. Different fixations have been tried, none delivering a better result than the one mentioned in 4.5.1. It does however seem to have a better preserved cell wall than the HPF sample seen on the right of fig. 5.11. Some very bright spots in the centre of the cell are probably due to a lack of resin infiltration. Membranes within the cell also have inverted contrast. Light spots close to the membrane within the cell presumably indicate insufficient lipid retention. Preservation within the HPF sample is improved but not satisfactory. The cell wall is entirely bright and the cell membrane mostly lost. The nucleus can barely be identified by the additional folds due to inactivation of the nucleoporin NUP60. Other cellular components can barely be made out (arrows indicate what are supposed to be mitochondria). Lastly, both cells exhibit high granularity stemming from post-staining procedures.

A cell that had not undergone post-staining is visible in fig. 5.12. It shows more detail, suggesting the cell was sufficiently stained during freeze substitution. Despite this, most cellular material was extracted in the fixation process.

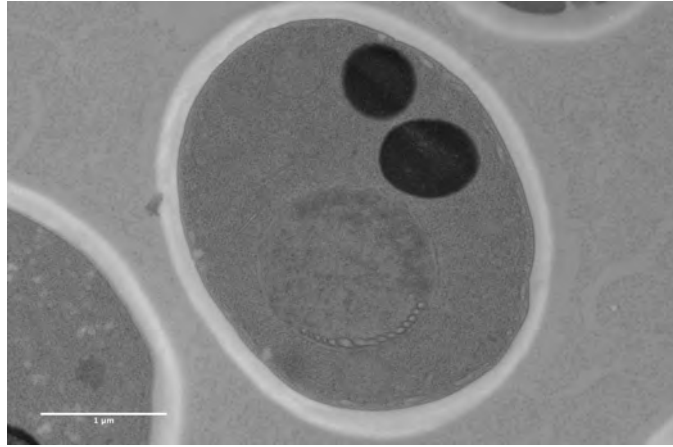


Figure 5.12: Unstained section of NUP60 yeast cell at 22 000x magnification. Scale bar of 1 μ m.

5.2 Artefacts

Especially regarding the preparation of biological samples, artefacts are an important aspect to take into account. They can form in almost every step of fixation. Buffer can form precipitates with fixatives, osmication can produce osmium blacks which strongly scatter electron radiation. Damage may occur during freezing or during transfer to the AFS. If the AFS temperature fluctuates or is not set properly, the cubic ice in the sample may recrystallise to hexagonal ice, distorting the sample in the process. Dehydration in the wrong solvent or an improper duration can lead to extraction of cellular components. Improperly mixed resin mixtures can separate and produce uneven infiltration. Sectioning may take a toll on the sample, for instance resulting in streaks, knife marks or holes. Finally, post-staining can affect the sample negatively, by adding precipitates.

Although artefacts are generally bothersome, they can give information on how to improve the chosen fixation method. Nevertheless, it is vital that artefacts are recognised appropriately and not used for evaluation of biological ultrastructure.

6. Discussion

When comparing CF and HPF-FS as methods of fixation, one cannot be said to universally be the better one. There are differences within one single sample, for example in the case of *C. elegans* where individual smooth muscle filaments can be clearly distinguished in the HPF sample but synapses are more visible and recognisable after CF. The choice of methods should therefore mainly depend on the area of interest being imaged.

The evaluation and comparison of methods can generally lead to improvement. The advantage of chemical fixation is its low cost and accessibility to users. It may also allow the fixation of larger sample than HPF would. Samples submitted to CF had undulated membranes that either appeared swollen or showed loss of the lipid bilayer. They looked more granular and had a greater tendency for problems during infiltration and embedding of resin. Mitochondria were excessively swollen and exhibited similar damages as membranes. Noticeable in the case of *C. elegans* was the improved preservation of synapses around the worm's mouth. CF samples presented more embedding deficits such as holes, tears and streaks in the resin.

High-pressure freezing is a method containing many more variables within a broader range. It requires additional, and unfortunately, expensive equipment and more experience. Developments in machinery however aim to reduce the involvement of the user and to increase automation of the process. Specimen handling before and after freezing could be automated, as well as the transfer to automatic freeze substitution. HPF can thus be considered the method with a higher potential of improvement over the next few years. Another advantage of HPF is the ability to freeze samples at a certain point in time and selectively freeze-substitute them. Once frozen, samples can

be stored in LN₂ indefinitely without causing damage to the sample. HPF also minimises or even eliminates movement of the specimen during fixation, as opposed to CF. Different FS protocols can then be tried out with only one HPF run-through. Membranes in HPF-FS samples proved to be much smoother and the lipid bilayer was preserved. Layers of the *C. elegans* cuticle were better resolved. Mitochondria also were smoother and did not aggregate. Muscle filaments, both transversal and longitudinal to the image plane, were better preserved. Viruses were clearly identifiable in the HPF sample of HeLa cells but not after CF. However, HPF samples generally made a more inflated impression. In most cases, resin embedding was visibly improved compared to CF samples.

This is consistent with observations made in the referenced literature, where smoother membranes and swollen organelles were noticed. Other works, such as [6], also mention that HPF offers better fixation in the presence of a thicker cuticle. Smoother membranes after HPF-FS were described by authors of [2], [3] and [5]. Kaneko and Walther too note swollen organelles after high-pressure freezing and freeze substitution in [4].

One of the main difficulties that surfaced was to find the same object in both samples. Multicellular organisms are much more complex which aggravates this problem. The same area must be found and it should also be in the same stage of development. Several sections of *Caernohabditis elegans* had to be produced in order to be able to find sections appropriate for comparison. Naturally two different worms had to be used for method comparison, and obvious differences such as the presence of *E. coli* in the mouth are present. It also cannot be said for sure that the exact same part of the nematode are imaged. Also, as visible with *Drosophila testes*, it is a challenge to find spermatocysts in the same stage of development in CF and HPF specimens. For the above reasons, viruses (seen here in HeLa cells) and prokaryotic cells (such as cyanobacteria) are more suitable subjects for comparison. Nevertheless, it is also necessary to compare methods for eukaryotic cells and larger, more complex organisms and tissues.

An additional hindrance would be differences in brightness that occur when imaging the samples. The camera used might be set up to register

a specific count and not allow to draw conclusions to the average electron density of the sample. This can be observed in certain images appearing notably darker than others, although the same imaging parameters were used.

Taking all experiments of this thesis into account, HPF showed to in general be the preferable method for improved structural preservation and detail compared CF. Nevertheless, the method of fixation must always be chosen according to the structure and organism being imaged.

7. Outlook

Ideally, it would be possible to determine the best fixation method for every single type of specimen, implying more work being done on the comparison of methods. Patterns and tendencies observed in this work can be checked and hopefully confirmed by analysing a variety of other samples. For specimens requiring a great deal of information, it may prove useful to use both techniques in parallel. Thus, details about the ultrastructure can be gained from several sources. This would allow eliminating wrongful interpretation of artefacts and obtaining different perspectives on the same specimen.

High-pressure freezing and freeze substitution methods are subject to continuous development and therefore probably are a great source of improvement when it comes to fixation of biological samples. Another possibility is to combine both methods, by high-pressure freezing samples pre-fixed using glutaraldehyde. This could combine advantages of both techniques but also lead to their respective artefacts adding up.

Bibliography

- [1] H. Moor. Theory and Practice of High Pressure Freezing. In *Cryotechniques in Biological Electron Microscopy*, chapter 8, pages 175–191. Springer Berlin Heidelberg, Berlin, Heidelberg, 1987.
- [2] B. Zechmann, M. Müller, and G. Zellnig. Effects of different fixation and freeze substitution methods on the ultrastructural preservation of ZYMV-infected *Cucurbita pepo* (L.) leaves. *Journal of Electron Microscopy*, 54(4):393–402, 2005.
- [3] J. Z. Kiss, T. H. Giddings, L. A. Staehelin, and F. D. Sack. Comparison of the ultrastructure of conventionally fixed and high pressure frozen/freeze substituted root tips of *Nicotiana* and *Arabidopsis*. *Protoplasma*, 157:64–74, 1990.
- [4] Y. Kaneko and P. Walther. Comparison of ultrastructure of germinating pea leaves prepared by high-pressure freezing-freeze substitution and conventional chemical fixation. *Journal of electron microscopy*, 44(2):104–109, 1995.
- [5] S. M. Royer and J. C. Kinnamon. Comparison of high-pressure freezing/freeze substitution and chemical fixation of catfish barbel taste buds. *Microscopy Research and Technique*, 35(5):385–412, 1996.
- [6] D. Serwas and A. Dammermann. Ultrastructural analysis of *Caenorhabditis elegans* cilia. In R. Basto and K. Oegema, editors, *Methods in Cell Biology*, volume 129, chapter 18, pages 341–367. Elsevier Inc., Vienna, 2015.

- [7] S. Tsuyama, S. Matsushita, T. Takatsuka, S. Nonaka, K. Hasui, and F. Murata. Cytochemical investigation of gastric gland component cells with high-pressure freezing followed by freeze-substitution and hydrophilic resin embedding. *Anatomical Science International*, 77(1):74–83, 2002.
- [8] D. B. Williams and C. B. Carter. *Transmission Electron Microscopy*. Springer New York, 2nd edition, 2009.
- [9] F. Krumeich. Electron energy loss spectroscopy (eels). <http://www.microscopy.ethz.ch/EELS.htm>.
- [10] H. Bergwerf. Molview. <http://molview.org/>.
- [11] M. A. Hayat. *Principles and Techniques of Electron Microscopy*. Cambridge University Press, 4th edition, 2000.
- [12] P. M. Hardy, G. J. Hughes, and H. N. Rydon. Identification of a 3-(2-piperidyl)pyridinium derivative ('anabilysine') as a cross-linking entity in a glutaraldehyde-treated protein. *J. Chem. Soc., Chem. Commun.*, (21):759–760, 1977.
- [13] I. Migneault, C. Dartiguenave, M. J. Bertrand, and K. C. Waldron. Glutaraldehyde: behavior in aqueous solution, reaction with proteins, and application to enzyme crosslinking. *BioTechniques*, 37(5):790–802, 2004.
- [14] K.-E. Rasmussen and J. Albrechtsen. Glutaraldehyde. The Influence of pH, Temperature, and Buffering on the Polymerization Rate. *Histochemistry*, 38:19–26, 1974.
- [15] J. Coetzee and C. F. van der Merwe. Some characteristics of the buffer vehicle in glutaraldehyde-based fixatives. *Journal of Microscopy*, 146(2):143–155, 1987.
- [16] S. D. Russell. Buffers. <http://www.ou.edu/research/electron/bmz5364/buffers.html>.

- [17] International Association for the Properties of Water and Steam. Why does water expand when it freezes? <http://www.iapws.org/faq1/freeze.html>.
- [18] H. T. Meryman. Freezing injury and its prevention in living cells. *Annual Review of Biophysics*, (237):341–363, 1974.
- [19] K. Muldrew and L. E. McGann. Mechanisms of intracellular ice formation. *Biophysical Journal*, 57:525–532, 1990.
- [20] D. E. Pegg. *Principles of Cryopreservation*, volume 1257, chapter 1, page pages.
- [21] H. Kanno, R. J. Speedy, and C. A. Angell. Supercooling of Water to -92 degrees C Under Pressure. *Science (New York, N.Y.)*, 189(4206):880–881, 1975.
- [22] M. Chaplin. Ice phases. http://www1.lsbu.ac.uk/water/ice_phases.html.
- [23] R. Dahl and L. A. Staehelin. High-pressure freezing for the preservation of biological structure: Theory and practice. *Journal of Electron Microscopy Technique*, 13(3):165–174, 1989.
- [24] Cavit. Ice III phase diagram. https://commons.wikimedia.org/wiki/File:Ice_III_phase_diagram.svg.
- [25] MedSynapses. Microtome. <https://www.medsynapses.com/2012/02/microtome.html>.
- [26] The-Crankshaft Publishing. Caenorhabditis (molecular biology). <http://what-when-how.com/molecular-biology/caenorhabditis-molecular-biology/>.
- [27] B. Speers. Introduction to the cyanobacteria. <http://www.ucmp.berkeley.edu/bacteria/cyanointro.html>.

- [28] B. Speers. Cyanobacteria: Life history and ecology. <http://www.ucmp.berkeley.edu/bacteria/cyanolh.html>.
- [29] C. Smith. Cyanobacteria. <http://www1.biologie.uni-hamburg.de/b-online/library/webb/BOT311/Cyanobacteria/Cyanobacteria.htm>.
- [30] GreenWater Laboratories. Algae and cyanobacteria. <http://greenwaterlab.com/algae-cyanobacteria.html>.
- [31] O. Ciferri. Spirulina, the Edible Microorganism. *Microbiological Reviews*, 47(4):551–578, 1983.
- [32] Cyanosite. Cyanobacterial image gallery. <http://www-cyanosite.bio.purdue.edu/images/lgimages/ARTHROS1.JPG>.
- [33] UTEX. Utex 625. <https://utex.org/collections/living-algal-strains-test/products/utex-0625>.
- [34] Flymove. <http://flymove.uni-muenster.de/>.
- [35] L. Margaritis, F. Kafatos, and W. Petri. The eggshell of *Drosophila melanogaster*. I. Fine structure of the layers and regions of the wild-type eggshell. *Journal of Cell Science*, 43(1), 1980.
- [36] B. E. Staveley. Model organism: *Drosophila melanogaster*. http://www.mun.ca/biology/desmid/brian/BIOL3530/DEVO_02/ch02f01.jpg.
- [37] T. Morgan. Sex limited inheritance in *Drosophila*. *Science*, 32(812):120–122, 1910.
- [38] E. Callaway. Deal done over HeLa cell line. *Nature*, 500:132–133, 2013.
- [39] Cold Spring Harbor. CSK buffer. *Cold Spring Harbor Protocols*, 2007(11), 2007.